GEAP-5086
JANUARY 1966

EURAEC
JOINT U.S.-EURATOM RESEARCH
AND DEVELOPMENT PROGRAM

PRESTRESSED CONCRETE PRESSURE VESSELS FOR BOILING WATER REACTORS

SECOND QUARTERLY REPORT OCTOBER - DECEMBER 1965

U.S. ATOMIC ENERGY COMMISSION
CONTRACT AT(04-3)-189
PROJECT AGREEMENT 46

R+D.

ADVANCED PRODUCTS OPERATION
GENERAL ELECTRIC
SAN JOSE, CALIFORNIA

DISCLAIMER

EURAEC
GEAP-5086
Joint U.S. - Euratom Research
and Development Report
January 1966

PRESTRESSED CONCRETE PRESSURE VESSELS FOR BOILING WATER REACTORS

CFSTI PRICES

H.C. $3.00 ; MN .65

SECOND QUARTERLY REPORT
OCTOBER - DECEMBER 1965

Compiled by: G. Boggio

Approved: P. M. Murphy
Project Engineer

U.S. Atomic Energy Commission
Contract AT(04-3)-189
Project Agreement 46

Printed in U.S.A. Available from the
Clearing House for Federal Scientific and Technical Information
National Bureau of Standards, U.S. Department of Commerce
Springfield, Virginia
Price: $3.00 per copy

ADVANCED PRODUCTS OPERATION
GENERAL ELECTRIC
SAN JOSE, CALIFORNIA

2824-APA-76
100-wdh-1/66

LEGAL NOTICE

THIS DOCUMENT WAS PREPARED UNDER THE SPONSORSHIP OF THE ATOMIC ENERGY COMMISSION PURSUANT TO THE JOINT RESEARCH AND DEVELOPMENT PROGRAM ESTABLISHED BY THE AGREEMENT FOR COOPERATION SIGNED NOVEMBER 8, 1958, BETWEEN THE GOVERNMENT OF THE UNITED STATES OF AMERICA AND THE EUROPEAN ATOMIC ENERGY COMMUNITY (EURATOM). NEITHER THE UNITED STATES, THE U.S. ATOMIC ENERGY COMMISSION, THE EUROPEAN ATOMIC ENERGY COMMUNITY, THE EURATOM COMMISSION, NOR ANY PERSON ACTING ON BEHALF OF EITHER COMMISSION:

A. MAKES ANY WARRANTY OR REPRESENTATION, EXPRESS OR IMPLIED, WITH RESPECT TO THE ACCURACY, COMPLETENESS, OR USEFULNESS OF THE INFORMATION CONTAINED IN THIS DOCUMENT, OR THAT THE USE OF ANY INFORMATION, APPARATUS, METHOD, OR PROCESS DISCLOSED IN THIS DOCUMENT MAY NOT INFRINGE PRIVATELY OWNED RIGHTS; OR

B. ASSUMES ANY LIABILITIES WITH RESPECT TO THE USE OF, OR FOR DAMAGES RESULTING FROM THE USE OF ANY INFORMATION, APPARATUS, METHOD OR PROCESS DISCLOSED IN THIS DOCUMENT.

AS USED IN THE ABOVE, "PERSON ACTING ON BEHALF OF EITHER COMMISSION" INCLUDES ANY EMPLOYEE OR CONTRACTOR OF EITHER COMMISSION OR EMPLOYEE OF SUCH CONTRACTOR TO THE EXTENT THAT SUCH EMPLOYEE OR CONTRACTOR OR EMPLOYEE OF SUCH CONTRACTOR PREPARES, HANDLES, DISSEMINATES, OR PROVIDES ACCESS TO, ANY INFORMATION PURSUANT TO HIS EMPLOYMENT OR CONTRACT WITH EITHER COMMISSION OR HIS EMPLOYMENT WITH SUCH CONTRACTOR.

LN5

TABLE OF CONTENTS

LIST OF ILLUSTRATIONS

LIST OF ILLUSTRATIONS
(Cont)

INTRODUCTION

The United States and the European Atomic Energy Community (Euratom), on May 29, and June 18, 1958, signed an agreement which provides a basis for cooperation in programs for the advancement of the peaceful applications of atomic energy. This agreement, in part, provides for the establishment of a Joint U. S. - Euratom research and development program which is aimed at reactors to be constructed in Europe under the Joint Program.

The work described in this report represents the Joint U. S. - Euratom effort which is in keeping with the spirit of cooperation in contributing to the common good by the sharing of scientific and technical information and minimizing the duplication of effort by the limited pool of technical talent available in Western Europe and the United States.

SECTION I

SUMMARY

For the adaption of the boiling water reactor (BWR) systems to service with a prestressed concrete pressure vessel, a number of arrangements of natural and forced circulation BWR systems in both spherical and cylindrical vessels have been investigated. Cost and performance data are being accumulated for the selection of the most promising concept.

The results obtained in the reporting period are presented with particular regard to:

Vessel dimensions variation as function of reactor concept, power density, and vessel shape,

Core thermal-hydraulic performance for steady and dynamic states,

Coolant recirculation systems, and

Effect of reactor design pressure.

Research and development work performed on vessel thermal insulation is presented by describing the insulation materials and systems under consideration, the experimental equipment constructed to test the material properties, the insulation installation techniques, and the transpiration cooling system flow distribution.

SECTION II

STATEMENT OF PROBLEM

During the reporting period, work has concentrated on design and arrangement concepts of a number of natural- and forced-circulation BWR (NCBWR and FCBWR) systems for service in both spherical and cylindrical vessels.

The items considered to have the most influence on the differential capital cost among the many combinations are:

Reactor vessel, vessel liner and cooling system;

Vessel thermal insulation;

Reactor equipment;

Reactor external building;

Turbine generator set; and

Coolant recirculation equipment.

The variable parameters considered important to the survey are: active fuel length, reactor power density, reactor operating pressure, and number of fuel rods per fuel assembly. The relationships existing among all the variables are shown in Figures 5-1 and 5-2.

For each one of the different combinations of the variable parameters chosen, a reactor design is established for which the above items are set and their costs evaluated. Cost items other than the above are assumed not to influence the relative comparison of the design concepts.

For the fuel cycle costing, initial fuel enrichment, final enrichment, and plutonium yield are evaluated for each reactor design as functions of its average core void fraction and dimensions. From these values, the use charge, uranium depletion, and plutonium credit are accordingly computed. Fuel fabrication cost varies, depending on fuel length and number of rods required per bundle.

SECTION III

TECHNICAL PROGRESS

The presentation of work accomplishment follows the task breakdown described in the first quarterly report.

3.1 TASK I - INITIAL CONCEPTUAL DESIGN STUDY

3.1.1 Subtask I-2 - System Concepts

3.1.1.1 Introduction

For the reactor design concepts considered, detailed investigations have been carried out on reactor arrangements. Graphs have been prepared showing vessel dimension (inside insulation) as a function of active fuel length, power density, and, for natural circulation, of chimney length.

Core thermal-hydraulic calculations, although not completed, are at an advanced stage of progress. Partial results are reported, especially for the natural circulation system which is requiring, for the novelty of the design, greater attention than the more standard forced circulation system.

Plant efficiency variation as a function of heat loss through vessel insulation, reactor operating pressure, and pumping power has been prepared, as has the variation of the pumping power as a function of reactor pressure drop and core exit quality. Cost of reactor equipment, pump equipment, turbine-generator set, and reactor building are being estimated for use in determining the net cost differential between the different reactor systems.

Work accomplishments to date are reported in detail below.

3.1.1.2 Reactor Arrangements

Arrangement studies have continued during the reporting period to determine configuration and pertinent dimensions of reactor vessel internals as a function of reactor core parameters and coolant system characteristics and to determine the effect of the resulting internal arrangements on reactor vessel internal dimensions. The previous quarterly report showed sketches typifying the various arrangement concepts under study and discussed some of the factors which influence the reactor vessel size. This report presents sketches typifying in greater detail the various concepts under consideration. Also presented are curves showing the important dimensions of reactor components and the reactor vessel internal dimensions as a function of active fuel length over a power density range of 30 to 40 kW/l (assuming a reactor thermal power of 3170 MWt which would correspond approximately to a net electrical power of 1000 MWe). The data obtained from the arrangement studies are being used in the economic evaluation of the various concepts as reported in the next section.

Figure 5-3 shows reactor size data including core equivalent diameter, core circumscribed diameter, shroud diameter, and elevation of outermost fuel channel above vessel insulation as a function of active fuel length for 40 kW/l power density.

The inside height of a cylindrical vessel is influenced by the refueling space requirement and the arrangement of internals such as dryers, steam separators, and chimneys. Figure 5-4 shows the vessel height required inside the thermal insulation as a function of active fuel length for two cases of chimney height for a concept using free surface steam separation (total chimney height is defined as the distance from the top of the active fuel to the top of the chimney and includes 1.3 feet of fuel channel, i.e., the distance between the top of the active fuel and the bottom of the chimney structure). The figure shows that where no chimney structure exists above the fuel channel, i.e., for the case of forced circulation, steam dryer considerations determine the vessel height except for the longer cores. For a concept utilizing a chimney of significant length, refueling considerations determine the vessel height except for the shorter cores.

Figure 5-5 shows cylindrical vessel height and diameter inside the thermal insulation for the concept of mechanical steam separation and for two cases of separator location:

1. where the separators are located directly over the core and above the refueling space (Figure 5-6), and

2. where the separators are located around the periphery of the core structure and refueling space (Figure 5-7).

Separators may be located peripherally at the expense of vessel diameter and a saving of height or they may be located over the core and above the refueling space at a saving of vessel diameter but at the expense of height and increased refueling machine length. An important consideration, however, is that of maintenance and replacement of equipment. The concept of over-core separators is much more desirable from that standpoint.

Figure 5-8 shows spherical vessel diameter as a function of active fuel length for the concepts using free surface steam separation. Over the fuel length range of greatest interest (8 feet to 12 feet) the vessel diameter is set by the headroom requirements for either refueling or dryers depending on the chimney length used. Only for fuel lengths less than 8 feet and for extremely short chimneys is the vessel diameter established by steam separation capability. The curves show that a change in power density from 30 kW/l to 40 kW/l will reduce vessel diameter by no more than about 1.5 feet.

Figures 5-6, 5-7, 5-9 through 5-14 are sketches illustrating most of the concepts under study. Figure 5-9 shows a concept of reactor in a cylindrical vessel utilizing forced circulation and free surface steam separation with jet pumps located adjacent to the core. Figure 5-10 shows a similar concept with a different type of jet pump located in the region below the core elevation. This concept of jet pump offers the promise of easier access to jet pump nozzles. When utilized in the concept having over-core separators, the vessel diameter will be approximately 1 foot greater than that shown on Figure 5-5.

Figure 5-11 shows a concept of reactor in a cylindrical vessel utilizing natural circulation and a chimney. Figure 5-6 shows a concept utilizing over-core mechanical steam separators and Figure 5-7 shows a concept utilizing peripheral steam separators. (Figure 5-5 shows, as previously mentioned, relative vessel size requirements for these two concepts).

Figures 5-12 and 5-13 illustrate spherical vessels with free surface separation and forced and natural circulation with chimney, respectively. (Figure 5-8 shows relative vessel size requirements for these two concepts).

The foregoing sketches have been presented to illustrate the relationships between reactor vessel internals and the reactor vessel. Few details of structure are shown beyond those necessary to establish the dimensional limits.

Figure 5-14 shows a typical arrangement of control rod drive and in-core flux monitor housings extending through the bottom of the reactor vessel into the control rod drive room. The drawing also shows the space required below the bottom head for the drive hydraulic piping which runs to the hydraulic system equipment cells adjacent to the reactor vessel and the space required below the drive housings for drive removal.

3.1.1.3 Economic Evaluation of Reactor Equipment

For cost comparison purposes, differential equipment and equipment installations costs are being accumulated for the various concepts and range of conditions under study. The components being costed within the reactor region include those whose number and/or size and configuration vary with change in core geometry, concept, or operating conditions such as pressure and core exit quality. The major items include the following.

1. Control rods and related equipment, including
   a. Drives
   b. Drive housings and components
   c. Drive hydraulic systems
   d. Guide tubes
   e. Fuel support-guide tubes
   f. Control rod followers
2. In-core flux monitor housings and guide tubes
3. Poison curtains
4. Fuel channels
5. Core support structure
6. Shroud
7. Top guide
8. Chimney

9. Pumps

10. Mechanical steam separators

11. Dryers

12. Miscellaneous, such as
    a. Steam and feedwater piping
    b. Flow baffles
    c. Core support structure
    d. Auxiliary cooling systems
    e. Refueling equipment
    f. Fuel orifices
    g. Dummy fuel elements

All items except 1.f., 8, 9, and 10 are used in all reactor concepts. Control rod followers and chimneys are limited to the natural-circulation concept, pumps to forced-circulation concepts, and mechanical steam separators, of course, to the concepts utilizing mechanical steam separation. The unit cost of the single components of Item 1, control rod and related equipment, does not vary significantly with active fuel length, therefore their total cost is almost proportional to their number, i.e., to the square of the core diameter. Reactor equipment costs strongly favor the longer core concepts having a smaller overall diameter and fewer fuel assemblies and control rods.

Poison curtain costs vary with core diameter and length. Core support structure costs increase with diameter of core, pressure drop across the core, and design load, the two latter factors favor particularly natural circulation systems.

In-core flux monitor housing and flux monitor guide tube costs vary as the square of the diameter. Dryer costs are essentially constant for all concepts and core sizes. Natural-circulation concepts trade pumps for chimneys and control rod followers and the free surface separation concepts lack steam separators.

Reactor concept and internal configurations influencing reactor vessel size consequently will have some influence on the size and height of the reactor building.

The partial equipment cost estimates obtained to date, although insufficient to draw a conclusion as for the most promising reactor system, show a significant advantage for tall cores.

3.1.1.4 Core Thermal-Hydraulics

Introduction. During the reporting period major emphasis for the core thermal-hydraulics was placed on the following:

Steady State Analysis

1. Effect of changing NCBWR design pressure from 800 to 1250 psia.

2. Effect of a variation of number of fuel rods per fuel assembly.

3. Developing characteristic curves for FCBWR cores.

Dynamic State Analysis

1. Stability analysis of NCBWR's.

2. Effect of subcooling variation on stability.

3. Hot channel stability analysis.

For the natural-circulation cores it has been found possible to change a design with an unacceptable stability margin to one that is acceptable by the addition of an orifice at the fuel channel entrance. The additional head loss incurred is made up by extending the chimney length. Thus the chimney heights presented in the steady-state section must be considered as preliminary. The same reasoning applies to the head losses shown for the forced-circulation cores. Although a thorough stability analysis has been completed for one design only (viz: 8 ft active fuel NCBWR at 1050 psia) the steady-state results of all designs examined are presented. The range of parameters covered to date for the steady state is shown in Table 3-1.

TABLE 3-1

THERMAL-HYDRAULIC PARAMETERS

	NCBWR	FCBWR
Core Pressure, psia	800, 1050, & 1250	1050
Core Power Density, kW/l	20 - 50	30 - 55
Core Inlet Subcooling, Btu/lb	10 - 30	25
Number of Channels per Chimney	1 or 4	(no chimney)
Number of Rods per Channel	64 and 49	64
Fuel Rod Outside Diameter, in.	0.481 and 0.550	0.496
Active Fuel Length, ft	6 - 10	10 - 12
Average Channel Exit Quality, %	9 - 16	8 - 15

Note the variation in core inlet subcooling for the case of the NCBWR. In the last quarter a constant value of 20 Btu/lb was assumed, which was selected to be exact at an average exit steam quality of about 10 percent, a feedwater temperature of 320°F, and steam carryunder of 1 percent. Actually the inlet subcooling will be a function of quality and carryunder. For a design employing free surface steam separation the carryunder in turn will be a function of quality, reactor flow, and system geometry (i.e., velocity in downcomer). The assumption of constant inlet subcooling was found to have a small effect on the steady state results. Over the range of power density and quality of interest the estimated chimney height was within ±5 percent. However, when the stability analysis showed great sensitivity to the ratio of single-phase to two-phase pressure drop, the carryunder and inlet subcooling were studied in more detail. Carryunder was predicted for various NCBWR design points by using operating data from the Humboldt NCBWR, and the effect on stability investigated. (Results are discussed in dynamic-state section). Again the previous results (with constant subcooling) were accurate enough to permit postponement of further detailed subcooling variation analysis until needed in Task II. For this reason the FCBWR's are also analyzed with a constant subcooling. The value of 25 Btu/lb was selected instead of 20 because this is the direction of subcooling values for cores with higher exit qualities.

Steady State Analysis

1. Effect of Operating Pressure

The characteristics of NCBWR's operating at pressures from 800 to 1250 psia are shown in Figures 5-15 and 5-16. Figure 5-15 shows the chimney height required as a function of the pressure and average channel exit quality for a reactor with an 8-foot fuel length, operating at an average power density of 40 kW/l. Higher pressure systems are seen to require longer chimney sections and are limited to operation at lower qualities by the critical heat flux ratio.

Figure 5-16 shows chimney height as a function of power density, core pressure, and exit quality. The pressure curves are drawn for a minimum critical heat flux ratio (MCHFR) of 1.7 at rated power. The region to the left (lower power density and/or quality) of the pressure curves is acceptable since the MCHFR would be greater than 1.7. The general effect of pressure is that a particular chimney height design can be run at a higher power density for a lower pressure, but with a penalty (in fuel costs) of higher exit quality.

2. Effect of Number of Rods Per Channel

It was planned to study the above in detail during Task II, the optimization of the reference design. However, two values of this parameter were investigated to visualize the magnitude of the variation it will create. The preliminary results are shown in Figure 5-17. The core design was one of 8-foot active fuel length operating at 1050 psia. Standard BWR fuel designs of 64 and 49 rods per bundle were investigated. The curves show the limit lines for a MCHFR of 1.7 and the influence on chimney height, power density, and exit quality. Note that the latter are shown as straight lines since only two points were calculated. The result is that the use of more rods per bundle allows a slightly higher power density but is accompanied by quite a sharp increase in exit quality. Thus, for example, a design with a 10-foot chimney and 49 rods per bundle could operate at 45 kW/l with an exit quality of 12.8 percent. The same chimney with 64 rods per bundle could have a 47 kW/l power density at an exit quality of 14.4 percent. Since the stability analysis is affected by rod diameter, the above results cannot yet be used for the optimization.

3. Characteristics of Forced Circulation Cores

From a thermal-hydraulics standpoint the main difference between the NCBWR core and the FCBWR core is that the latter does not employ control rod followers. This was discussed in some detail in the previous quarterly report. In brief review, the effect is that for a given water-to-fuel ratio the FCBWR core will have larger diameter rods (for the same number of rods per channel) and less flow area in the channel than the matching NCBWR core.

The results of the FCBWR are shown with core head loss as the principal dependent variable. In the steady-state analysis the actual method of forcing the circulation (i.e., type of pump) is of no consequence. Only when the stability is analyzed does the pump characteristic curve influence the results.

The type of steam separation also does not affect the preliminary results presented herein. Free surface steam separation will have carryunder as a function of quality, etc. As previously mentioned this is not varied for the current analysis. With mechanical steam separators the carryunder will be a constant (~0.2 percent) and the pressure drops incurred in the separators would simply be added to that of the cores which have been calculated.

Thus the "reactor flow head loss" shown in the curves here are only core pressure drops. Figures 5-18 and 5-19 show the head loss as a function of core power density and average channel exit quality for active fuel lengths of 10 and 12 feet respectively. For a core designed to a MCHFR of 1.7, higher power densities are seen to be accompanied by larger head losses and by lower exit qualities. The critical heat flux limits are cross plotted on Figure 5-20 where head loss is a function of power density, active fuel length, and exit quality. The values of exit quality are those only at the critical heat flux limit, and a straight dotted line is drawn between the two known values. As an example a head loss of 6 psi incurred in a 12-foot core would have a power density of 40 kW/l and an exit quality of 12.4 percent. The same head loss in a 10-foot core would have a power density of 47 kW/l and 11.1 percent exit quality.

Dynamic State Analysis

1. Stability Analysis of NCBWR's

The stability requirements of three basic reactor core types over a range of parameters are being investigated. The core types and their parameters are listed in Table 3-2.

TABLE 3-2

CORE TYPES BEING INVESTIGATED

Core Type	Active Fuel Length, ft	Bundle Size, rods/bundle	Operating Pressure, psi	Steam Separation	Power Density, kW/l
Natural Circulation	7-10	49 and 64	850 - 1250	Free Surface	30 - 50
Forced Circulation (Jet Pumps)	8-12	49 and 64	850 - 1250	Free Surface or Mechanical	30 - 55
Forced Circulation (Mechanical Pumps)	8-12	49 and 64	850 - 1250	Mechanical	30 - 55

This quarter the major effort has been concentrated on the stability requirements of the natural circulation core. The preliminary results for the forced circulation core using free surface steam separation are still inconclusive and will be presented in the next quarterly report.

Figure 5-21 is a graph showing the phase and magnitude margin curves for a natural circulation core at an operating pressure of 1050 psi with an 8-foot active fuel length and 49 rods per bundle.* Examination of Figure 5-21 shows that the magnitude margin criterion, 13 db, is easily attainable over a wide range of chimney heights, power densities, and exit qualities. But the phase margin criterion, 55°, is satisfied only at long chimney heights or low power densities.

The stability can be improved by orificing the core inlet to increase the water phase pressure drop. The pressure drop across the orifice can be supplied by:

1. pumping (forced circulation), or

2. increasing the elevation head through increases in the length of the chimneys.

The effect each of these has on the stability is discussed below.

a. Pumping.** If jet pumps are used to make up for the pressure loss across the orifice, it is necessary to distinguish whether the control rods have followers. Without followers it is more convenient to eliminate the chimneys and increase the pumping power accordingly. With followers the chimney lengths should equal the length of the core to take advantage of the vessel height available because of control rod followers requirement. By using an example from Figure 5-21, the effect orificing has on stability can be illustrated.

For a specific set of parameters:

Power Density (q) = 40 kW/l,

Exit Quality (χ_e) = 10.8 percent,

Chimney Length (L_c) = 10.2 ft, and

Active Fuel Length (L_a) = 8.0 ft,

the stability was found to be:

Phase Margin (PM) = 36.6°

Magnitude Margin (MM) = 14.8 db.

If the chimney length is reduced to the length of the core (8 feet), with jet pumps supplying the loss in elevation head (0.4 psi), the stability was found to be:

Phase Margin (PM) = 40.3°

Magnitude Margin (MM) = 13.9 db.

*See Figure 5-22 for 10-foot active fuel length and 64 rods/bundle.

**The combination of chimneys with pumps (forced circulation) is included under the natural-circulation core. Forced-circulation stability analysis is reserved for cores with no chimneys.

With the jet pumps supplying an additional 0.3 psi of pressure, for the orificing pressure loss, the phase margin increased to 55°, and the magnitude margin increased to 18.1 db.

These results are summarized in Table 3-3.

TABLE 3-3

EFFECT OF CHIMNEY LENGTH ON STABILITY

L_c, ft	Orifice head loss, psi	Additional Pumping, psi	PM, degrees	MM, db
10.2	0	0	36.6	14.8
8	0	0.4	40.3	13.9
8	0.3	0.7	55	18.1

L_a = 8 feet

b. Increasing the Elevation Head. Figure 5-23 is a graph of the phase and magnitude margins as a function of increasing chimney length (the increase in elevation head is used to make up for the pressure drop across the orifice). Again, it is relatively easy to satisfy the magnitude margin requirements; the phase margin presents the problem. The technique of orificing as a means of improving stability was studied in detail to determine its limitations. It was found that the phase margin versus orificing pressure losses reaches a maximum with additional orificing having no effect. For the case of 10-foot active fuel and 64 rods per bundle (Figure 5-24) it was found that the phase margin curve never reached the stability criterion, regardless of the amount of orificing.

Figure 5-25 shows the lengths of chimney required to meet the stability criteria for the parameters used in Figure 5-21, when channel inlet orificing is used. Figure 5-26 illustrates the phase margin with no orificing and with the necessary orificing to meet stability requirements along the minimum critical heat flux limit.

The effect core operating pressure, number of rods per bundle, and active fuel length have on stability is shown in Table 3-4. These preliminary results indicate that pressure has little influence on stability. It can also be observed in Table 3-4 that increasing the fuel length and/or increasing the number of rods per bundle, tends to decrease the stability. However, these general effects are still being studied for each specific case and require additional analysis before any final conclusion can be made about their effect on stability.

TABLE 3-4

STABILITY OF VARIOUS CORES

L_a, ft	Rods/Bundle	Pressure, psi		
		800	1050	1250
8	49		χ_e = 10.5% PM = 28.4° MM = 10.9 db	
8	64	χ_e = 9.7% PM = 23° MM = 9.0 db	11% 22° 8.4 db	12.3% 23° 8.3 db
10	64		χ_e = 15% PM = 10.8 MM = 3.8 db	

Chimney Length = 5 feet
Power Density = 30 kW/l

2. Effect of Subcooling Variation on Stability

The preceding stability analysis is based on the assumption that the inlet subcooling is constant for a given pressure regardless of the steam exit quality. The validity of this assumption was tested along the minimum critical heat-flux limit in Figure 5-26 for the specific case where:

Active fuel length (L_a) = 8 ft,

Number of rods/bundle (Nrb) = 49,

Power Density (q) = 40 kW/l, and

Pressure (P) = 1050.

The two values of subcooling considered were 20 and 25 Btu/lb; 20 Btu/lb is the constant previously assumed and 25 Btu/lb is the value calculated to keep the feedwater temperature within a limited range of values.

The effect subcooling has on stability is illustrated in Table 3-5.

The difference in chimney lengths for the two cases, as determined by stability considerations, was found to be 0.15 ft. This difference is sufficiently small that the assumption of constant subcooling can be taken as valid for the Task I study.

TABLE 3-5

EFFECT OF SUBCOOLING ON STABILITY

Subcooling, Btu/lb	Without Orificing: λ_e, %	Without Orificing: Chimney Length, ft	Without Orificing: Stability	With Orificing at PM = 55°
20	14.7	5.62	PM = 25.2° MM = 10.1 db	L_c = 9.85
25	14.5	5.42	PM = 19° MM = 7.5 db	L_c = 10.0

3. Hot Channel Stability Analysis

The stability analysis is carried out on the average channel, nevertheless for chosen design points a check is carried out on the hot channel.

The present stability criteria for the hot channel using a single channel analysis are:

Phase Margin $\gtrsim$ 40°, and

Magnitude Margin $\geq$ 6 db.

The stability of the hot channel was checked for the following case:

L_a = 8 ft	Subcooling = 25 Btu/lb
Nrb = 49	L_c = 10 ft
P = 1050 psi	Power Density = 40 kW/l.

The results of this case are presented in Table 3-6.

TABLE 3-6

RESULTS OF HOT CHANNEL STABILITY ANALYSIS

	CHFR in the Hot Channel	Phase Margin, degrees	Magnitude Margin, db
Average Channel, Core Inlet Orificing (+ 0.4 psi)	1.7	55	26.8
Hot Channel, Uniform Core Orificing	1.83	72	27.3
Hot Channel, with No Orificing	2.13	35	13.0

Examination of Table 3-6 indicates it is possible to reduce the orificing in the hot channel while still satisfying the stability criteria. This reduction in orificing would redistribute the flow across the core increasing the minimum critical heat flux ratio. Any increase in the minimum critical heat flux ratio is desirable, for this extends the acceptable range of exit qualities and power densities.

3.1.1.5 Mechanical Steam Separation

The standard BWR axial flow separators located either in a peripheral manner as shown on Figure 5-7 or above the core as shown on Figure 5-6 provide a region above the core which is essentially free of obstructions during refueling. Both of these concepts will be considered in the optimization study.

Figure 5-27 shows the relationship between the core exit quality, number of separators required, and the total separator pressure drop.

3.1.1.6 Coolant Recirculation Pumps

Jet Pumps

Figure 5-28 shows the relationship between pumping power and core exit quality for 10 psi of pump head, for the free-surface-separation concept, and for the axial-separator concept. The difference between the curves is caused by the fact that the carryunder in the free-surface-separation concept varies with the core exit quality while the carryunder occurring in the mechanical-separation concept can be assumed to be a constant.

Recent jet pump tests under hot water conditions indicate that suction flow subcooling is not required for jet pumps operating under high pressure hot water conditions, and that the pumps operate equally well while pumping saturated 1000 psia water. Since the suction flow subcooling is obtained by using a fraction of the feedwater flow, lowering the subcooling requirement allows a larger fraction of the feedwater flow to be used as the driving flow, thus lowering the M ratio ($M = \frac{\text{suction flow}}{\text{driving flow}}$) and increasing the efficiency of the jet pump. Taking advantage of the effect, Figure 5-28 was plotted with the assumption that the suction flow was cooled only to the saturation point, i.e., the carryunder was condensed, but not subcooled.

For the present concepts, feedwater-driven jet pumps seem particularly advantageous because they allow the elimination of recirculation loops. However, feedwater-driven jet pumps have higher M ratios than the pumps currently being used for commercial BWR's and correspondingly higher nozzle velocities (600 versus 200 ft/sec). Although no tests have yet been conducted on the rate of nozzle erosion at these conditions, there is a possibility that nozzle wear in feedwater-driven jet pumps could be serious enough to require a pump design which would allow an easy replacement of the pump nozzles. It was for the above reason that the concept shown in Figure 5-10 was devised. In this system the jet pumps are placed in an inverted position around the periphery of the core. The nozzles would fit inside the feedwater pipe like pistons with holes in them; the driving flow would hold the nozzles in place. The removal of the nozzles would be accomplished by shutting off the driving flow and allowing the nozzles to drop down through the feedwater pipe out of the vessel into the drywell area where they can be replaced. This concept, while facilitating the replacement of the jet pump nozzles, would be more costly both from a hardware and vessel size standpoint, and therefore would not be used unless future tests indicated nozzle erosion was a serious maintenance problem.

Mechanical Pumps

Figure 5-29 shows the relationship between pumping power, core exit quality for 10 psi of pump head for both the free-surface and the mechanical steam separation concepts. The difference in the curves is caused by the variation in carryunder between the concepts; the free-surface-steam-separation concept having a higher carryunder requires a higher coolant flow and therefore a higher pumping power.

3.1.2 Subtask I-3 - Reactor Pressure Variation

The influence of reactor operating pressure on the economic evaluation of the different reactor concepts is being investigated with particular regard to thermal-hydraulic effects (see Section 3.1.1.4), plant efficiency, steam superficial velocity in the case of free surface steam separation, and turbine-generator cost. The variation of plant efficiency can be seen in Figures 5-30, 5-31, and 5-32 where the net electrical output is plotted versus the pumping power and heat loss through thermal insulation, respectively, for pressure values of 800, 1050, and 1250 psia. Figure 5-33 shows the variation of the superficial steam velocity, permissible steam release rate, and heat release rate as a function of reactor pressure; such variation influences the diameter of the cylindrical vessel of the free surface separation concept.

The trend of the above curves favors the higher reactor pressures; nevertheless the savings which would result will have to be compared with the additional cost of the concrete pressure vessel.

3.1.3 Subtask I-4 - Construction Schedule

For reactor system and vessel shape selection purposes the relative effect on reactor design of the construction schedule and acceptance testing sequence of the concrete vessel designs appears to be negligible. Such effects will be taken into account in Task II for the establishment of a reference design.

3.1.4 Subtask I-5 - Vessel Thermal Insulation

In the reporting quarter a test rig has been designed and constructed for determining material properties for both static- and transpiration-cooling systems. Furthermore, investigations have been performed for special problems such as heat transfer near vessel penetrations, installation techniques, and flow maldistribution in transpiration cooling caused by elevation head.

The insulation material types taken into consideration are basically "porous" stainless steel and are described in the first quarterly report.

The sintered random wire mesh (Figure 5-34) and the laminated embossed foil (Figure 5-35) will be tested for use as a static insulation. Sintered powder (Figure 5-36) and sintered woven wire (Figure 5-37) will also be tested as a static insulation; however, they are intended primarily as transpiration cooling materials. Unsintered woven wire and unsintered random wire mesh will also be tested. The unsintered wire materials are much less costly than the sintered wire materials but are not expected to be as resistant to corrosion. Since each of the above materials has its own advantages and disadvantages, a composite insulation of two or more types may prove to be the most promising.

The materials used in the transpiration cooling tests will be sintered powder, sintered woven wire, sintered random wire, combinations of the above, and the above materials combined with unsintered woven wire and/or unsintered random wire mesh. Material used as a porous medium for transpiration cooling must possess two characteristics: It must have a large internal surface area for heat transfer and it must provide sufficient pressure drop to the coolant flow to insure uniform flow distribution over the surface.

Probably the most widely used material for transpiration cooling is a multilayer sintered woven wire. Figure 5-38 shows an enlarged section of the surface of the material in the as-sintered condition.

Sintered woven wire is quite costly, but its advantages in transpiration cooling lie in its high resistance to corrosion and its easily controllable density. A material rolled to a relatively high density will provide a higher pressure drop to coolant flow but will also have a correspondingly higher thermal conductivity.

Preliminary investigation indicates that a transpiration medium consisting of laminations of two or more materials would be most desirable. A thin layer of high-density sintered woven wire on the reactor side would provide sufficient pressure drop and resistance to corrosion and a thicker layer of less-costly material (sintered or unsintered random wire mesh or unsintered woven wire) on the concrete side would provide a large internal surface area for heat transfer.

Analysis of the heat transfer in the region of vessel penetrations indicates that rounded edges on the penetration junctions should be considered, unless they are structurally very difficult to design. The heat transfer rate on a sharp corner is much higher than that on a flat wall, necessitating more cooling lines on the penetration junctions. However, if the edges can be rounded, the "corner" heat loss can be reduced considerably.

3.1.4.1 Experimental Program

The experimental program sequence for evaluation of static cooling materials and transpiration cooling systems will be as follows:

1. Atmospheric-pressure test of thermal conductivity of static-cooling materials.

2. High-pressure (1000 psia) test of thermal conductivity of static-cooling materials.

3. Atmospheric-pressure test of transpiration-cooling heat transfer.

4. High-pressure (1000 psia) test of transpiration-cooling heat transfer.

The atmospheric tests have two functions: To shake down the experimental equipment, and to obtain data with water having different transport properties. The first such test will be conducted with the static-cooling test equipment. The experimental technique will be to use the same equipment which will later be used inside the 1000 psia pressure vessel, immersing it in a tank of water open to the atmosphere.

3.1.4.2 Test Equipment for Static-Cooling System

Figure 5-39 shows the internal device to be used for low-pressure testing installed in the pressure vessel. Figure 5-40 is a cross section showing more detail of the test device, whose function is to determine the effective thermal conductivity of a sample of material. The samples will be 7 1/2 inches in diameter and 2 inches thick. Figure 5-41 is a detail drawing of the conduction block. The purpose of the conduction block is to determine the heat flux passing through the test sample by measuring the temperature gradient through the conduction block, since the heat flux in the conduction block is the same as the heat flux in the sample. The temperature gradient in the conduction block is measured by thermocouples imbedded in it.

The finned surface on the backside of the conduction block provides a path for the cooling water to carry away the heat which is transferred through the test sample and conduction block. A photograph of the conduction block (Figure 5-42) shows the milled slots through which the coolant will flow. Figure 5-43 shows a photograph of the complete heat transfer devices, exclusive of insulation and thermocouples. Figure 5-44 shows the 14-inch-i.d. pressure vessel during construction. The vessel will be capable of operation at 1200 psi, 600°F. Note that the test equipment was designed so that two samples can be installed in the pressure vessel at once. This was done to expedite the testing. Also, the pressure vessel will be mounted so that it can be rotated without being depressurized. This was done so that the entire range of face angles could be tested with a single setup. Since the face angle of the insulation changes throughout the spherical pressure vessel, it is important to determine the effect of inclination on the heat transfer properties.

3.1.4.3 Transpiration Cooling Flow Distribution

Transpiration cooling is being investigated as an alternate method for insulating the concrete pressure vessel. This technique consists of slowly seeping water through a matrix of porous stainless steel, counter to the direction of the flow of heat. The advantages of this cooling technique are:

1. Reduced complexity of cooling system: No special heat exchangers required, less piping and fewer pumps; and

2. Lower heat losses than for static cooling.

Problems which arise in the application of transpiration cooling are:

1. Possibility of porous material acting as a filter and becoming clogged over an extended period of time, and

2. Difference of elevation head can cause a problem of maldistribution of flow.

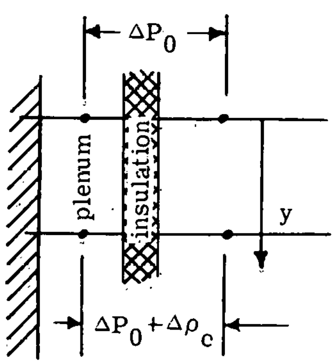

Consider the change in flow through a porous medium (sketch on preceding page) due to elevation head in the plenum for an NCBWR.

The flow rate at the datum plane is:

$$G_0 = \sqrt{\frac{2g\Delta P_0 \rho}{k}} .$$

The flow rate at some point, y, below the datum plane is:

$$G(y) = \sqrt{\frac{2\,g\Delta P\rho}{k}} = \sqrt{\frac{2g\rho\,(\Delta P_0 + \Delta P_e)}{k}}$$

$$G(y) = \sqrt{\frac{2g\rho(\Delta P_0 + \rho_e y)}{k}} .$$

For small y,

$$G(y) \approx \sqrt{\frac{2g\rho}{k}} \left(\sqrt{\Delta P_0} + \frac{1}{2}\,\frac{\rho_e y}{\sqrt{\Delta P_0}} - \frac{1}{8}\,\frac{\rho^2{}_e y^2}{\Delta P_0 \sqrt{\Delta P_0}} + \ldots\right);\ \frac{\rho_e y}{\Delta P_0} \ll 1$$

$$G(y) \approx \sqrt{\frac{2g\rho\Delta P}{k}} \left(1 + \frac{1}{2}\,\frac{\rho_e y}{\Delta P_0} - \frac{1}{8}\,\frac{\rho^2{}_e y^2}{\Delta P^2{}_0} + \ldots\right);\ \frac{\rho_e y}{\Delta P_0} \ll 1$$

Note that ρ_e is the net density difference between the coolant and the reactor fluid.

Define $G \equiv G_0\,(1 + \epsilon)$.

Then, for small y,

$$\epsilon = \frac{1}{2}\,\frac{\rho_e y}{\Delta P_0} - \frac{1}{8}\,\frac{\rho_e{}^2 y^2}{\Delta P^2{}_0} .$$

For moderate values of y, the first term dominates and the analysis is simplified to

$$\epsilon = \frac{1}{2}\,\frac{\rho_e y}{\Delta P_0} .$$

Solving for y:

$$y = \frac{2\,\Delta P_0 \epsilon}{\rho_e}$$

Hence, if ϵ is arbitrarily picked to be 10 percent, 20 percent, or whatever, the height at which this deviation occurs can be easily found, since ΔP_0 and ρ_e are known quantities.

Example:

$$\Delta P_0 = 1 \text{ psi},$$

$$\rho_e = (1/0.01634) \text{ lb/ft}^3, \text{ with water at } 150°\text{F},$$

$$\epsilon = 10\%,$$

$$y = 5.70 \text{ in.};$$

i.e., for 10 percent flow deviation,

$$y\ (10\%) = 5.70 \text{ in./psi with water } 150°\text{F}.$$

This analysis indicates that transpiration cooling of the Concrete Pressure Vessel should be limited to horizontal surfaces, or the region below the water line because of the change of available pressure drop across the material due to elevation head. The two alternatives to not using transpiration cooling in the steam region are:

1. Use very high pressure drop porous material.

   A. Use denser material (smaller pores), or

   B. Use thicker material.

2. Allow coolant flow rate to vary with height.

If less-porous material is used to get higher pressure drop, the risk of plugging the material is higher, since the material becomes a more effective filter. If thicker materials are used to increase the pressure drop, the cost is increased. In both cases, when the pressure drop is increased, pumping costs are increased.

If the coolant flow rate is allowed to vary from top to bottom, the flow rate at the water line below will be about 4 times that necessary for maintaining proper concrete temperature. This means a significant increase in required coolant flow, and a proportional increase in heat loss; e.g., if the coolant mass velocity increases linearally with height from its required value, G_0, at the top of a spherical vessel to 4 G_0 at the midpoint, and is constant 4 G_0 below that point,

The total flow rate is:

$$W = \int G dA = \int_0^{\pi/2} G(y)\ 2\pi r^2 \cos \theta d\theta\ +\ 4\ G_0\ 2\pi r^2 =$$

$$= 5\pi r^2\ G_0 + 8\pi r^2\ G_0 = 13\pi r^2\ G_0$$

The ideal coolant flow rate is $4\ \pi r^2\ G_0$, therefore the ratio of the two flow rates is $\frac{13}{4}$ or 3-1/4 times as much coolant flow for such a case. This also means 3-1/4 times as much heat loss, since for transpiration cooling, heat loss is directly proportional to coolant flow rate.

Unless this flow maldistribution problem can be solved, the transpiration-cooling technique must be limited to horizontal regions. Another possibility is to use transpiration cooling in local problem areas, such as vessel penetrations, or at structural supports.

3.1.4.4 Installation Techniques

The present technique envisioned for installation of the stainless steel insulation is to use material in panels of 4 × 8 feet × 1 inch, and to use three layers to get the required 3 inches of insulation. The sheets of insulation will be heliarc welded directly to the stainless steel liner and then to each other as shown in Figure 5-45. Basically there are two kinds of welds, Type "A" and Type "B". Type "A" welds the base of the insulation material to the material behind it. Type "B" welds, which weld the tops of two adjacent sheets of insulation, are necessary because the back of the sheet cannot be reached after the sheet is in place. The welds may be done two ways: either by welding the porous material directly, or if this isn't possible, by welding a stainless steel edging which is prefabricated with the insulation. The welding technique problem is to be investigated in detail during the next quarter.

Another item shown in Figure 5-45 is the special tack, the purpose of which is to support the insulation from sagging between the edge welds. These tacks will have an insulated shank about 3 inches long, with the point shaped to facilitate spot welding of the point to the stainless steel liner. The shank will be about 1/16-inch in diameter, insulated with a very thin coat of alumina. The purpose of the insulation is to prevent short circuits during the spot welding process. The heads of the special tacks will be insulated on the shank side and bare on the top side. The insulation on the head will also be a very thin coat of alumina. The thin alumina coat on these special tacks may not be required along the entire length of the shaft and bottom of the head. It is likely (depending upon the type of vessel insulation used) that only the region near the tip need be coated with alumina. The tip itself must be bare.

The installation technique, using these special tacks, is to drive them through the insulation material at preestablished spacings, until the point touches the stainless steel liner, then apply the spot welder to the bare top of the tack, welding the tack to the liner. Figure 5-45 shows a multiple layer of stainless steel screen covering the insulation material. This screen can be applied in very long rolls as the final layer of insulation. The main purpose of the screen is to retain the insulation material and block the flow of water to the spaces between sheets of insulation. An added benefit of the screen is that it will provide additional insulation.

SECTION IV

FUTURE WORK

In the next three months the work planned is as follows:

4.1 TASK I

4.1.1 A final choice will be made among the different design concepts on the basis of differential cost evaluation and technical feasibility. The technical parameters for the reference design to be developed in Task II will be selected.

4.2 TASK II - SUBTASK II-1

Work will be started for the adaptation of the reactor design chosen in Task I to the prestressed concrete pressure vessel concept. This task will be complete with reactor control rods and drives, coolant recirculation system, steam separation and drying equipment, and refueling equipment.

4.3 TASK III - SUBTASK III-2

Research and Development on vessel thermal insulation will be continued:

Experiments on material properties in static and transpiration cooling will be performed;

Test equipment for the experimental evaluation of specific problems will be constructed; and

A report of the conclusions of the first phase of the study will be prepared.

SECTION V

ILLUSTRATIONS

This section contains Figures 5-1 through 5-45.

NOMENCLATURE:

- Q_t = REACTOR THERMAL POWER, MWt
- E = FUEL EXPOSURE, MTU
- w/f = WATER-TO-FUEL RATIO
- L_a = ACTIVE FUEL LENGTH, Ft.
- L_c = CHIMNEY LENGTH, Ft.
- q = POWER DENSITY, kW/ℓ
- p = REACTOR OPERATING PRESSURE, psia
- r = NUMBER OF FUEL RODS PER BUNDLE
- X_e = CORE AVERAGE STEAM EXIT QUALITY, %
- E_g = GROSS ELECTRICAL OUTPUT, MWe
- E_n = NET ELECTRICAL OUTPUT, MWe
- E_p = PUMPING POWER, MWe
- Q_L = HEAT LOSS THROUGH VESSEL THERMAL INSULATION, MWt
- ϕ = HEAT FLUX THROUGH VESSEL THERMAL INSULATION, W/ft^2
- w = COOLANT FLOW REQUIRED BY TRANSPIRATION COOLING, lb/h
- U = OVER-ALL HEAT TRANSFER COEFFICIENT FOR VESSEL THERMAL INSULATION (Static cooling), Btu/h-ft^2 – °F

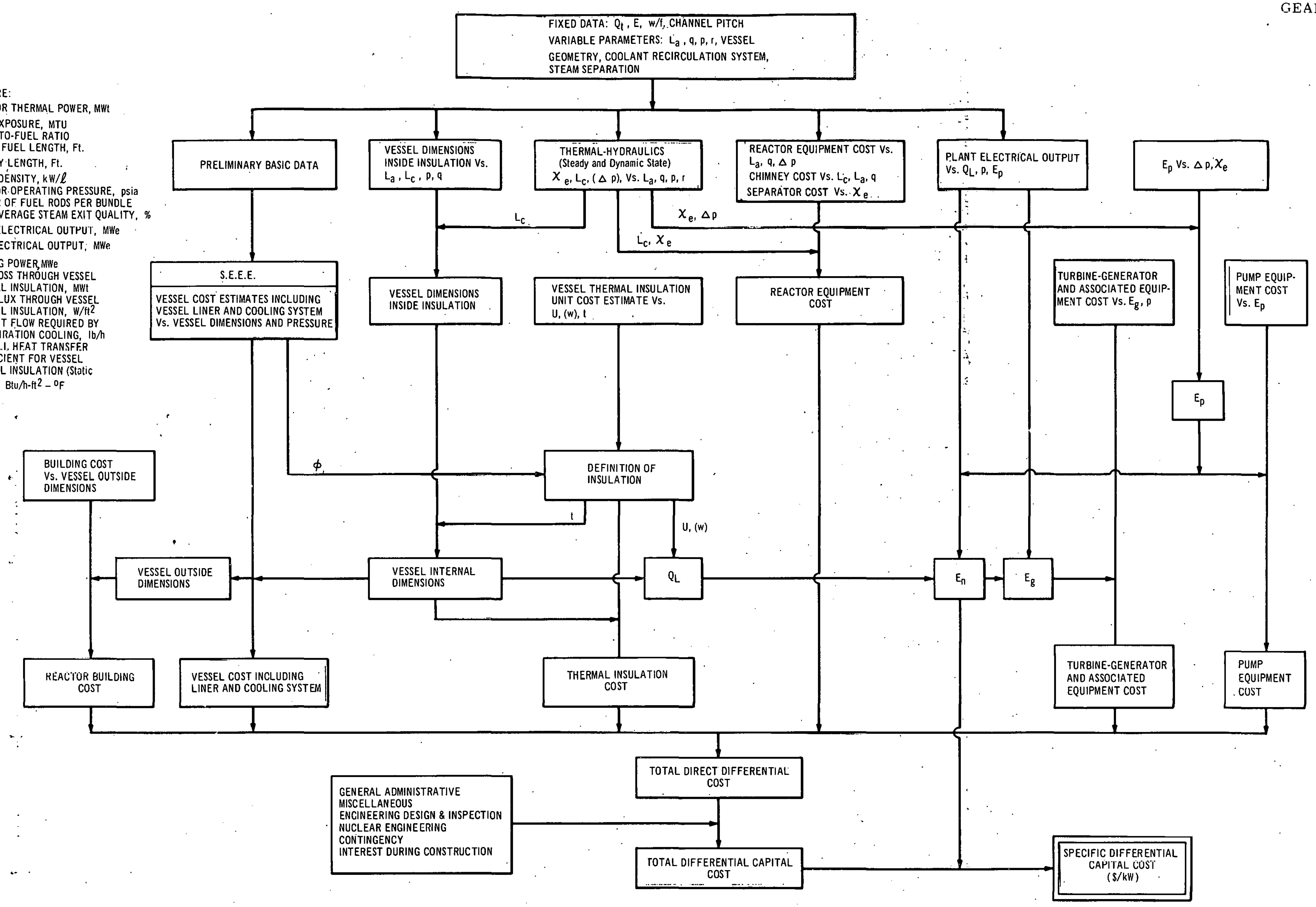

Figure 5-1. Block Diagram of Conceptual Design Study

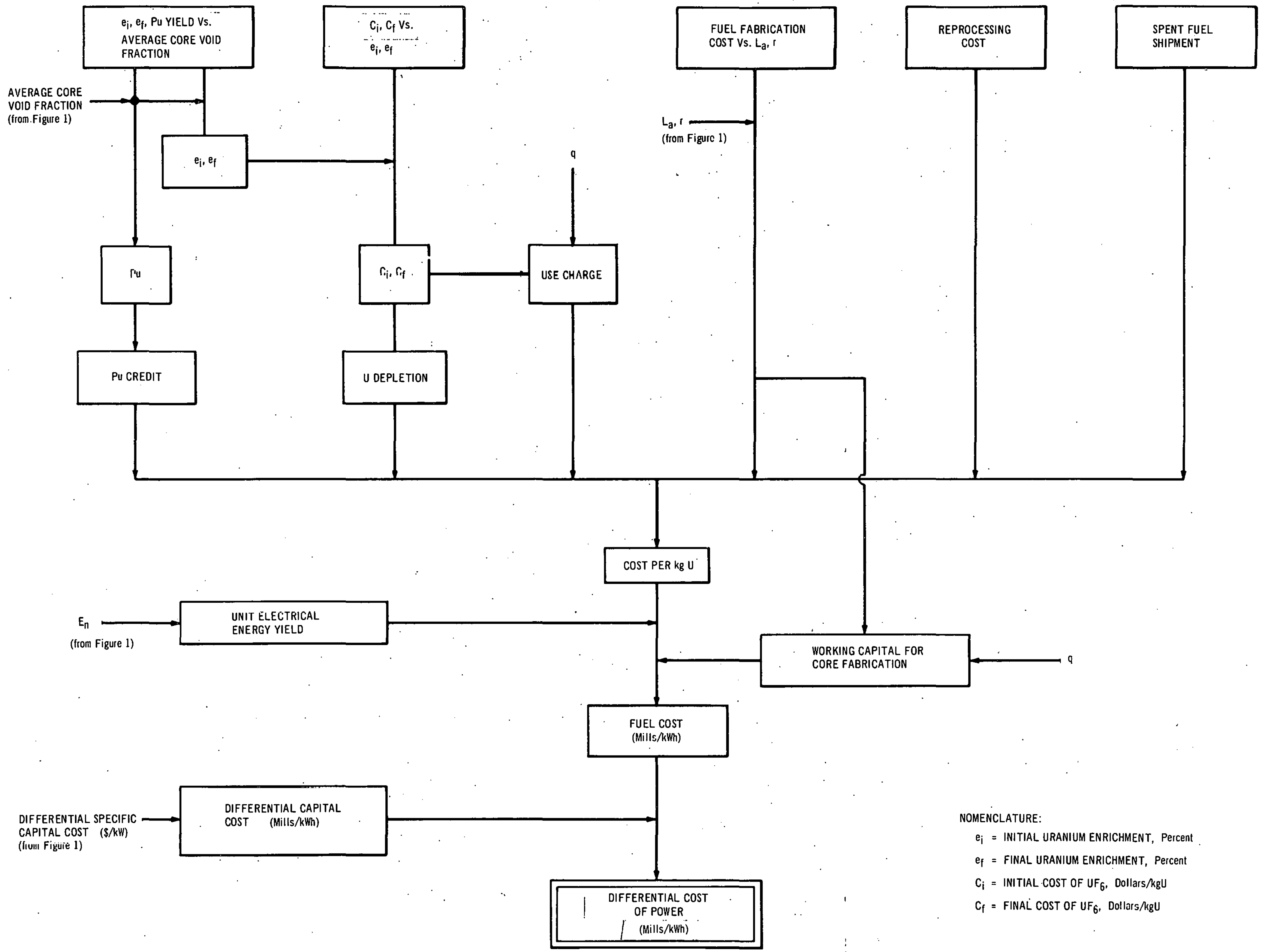

NOMENCLATURE:

e_i = INITIAL URANIUM ENRICHMENT, Percent

e_f = FINAL URANIUM ENRICHMENT, Percent

C_i = INITIAL COST OF UF_6, Dollars/kgU

C_f = FINAL COST OF UF_6, Dollars/kgU

Figure 5-2. Block Diagram of Fuel Cycle Cost

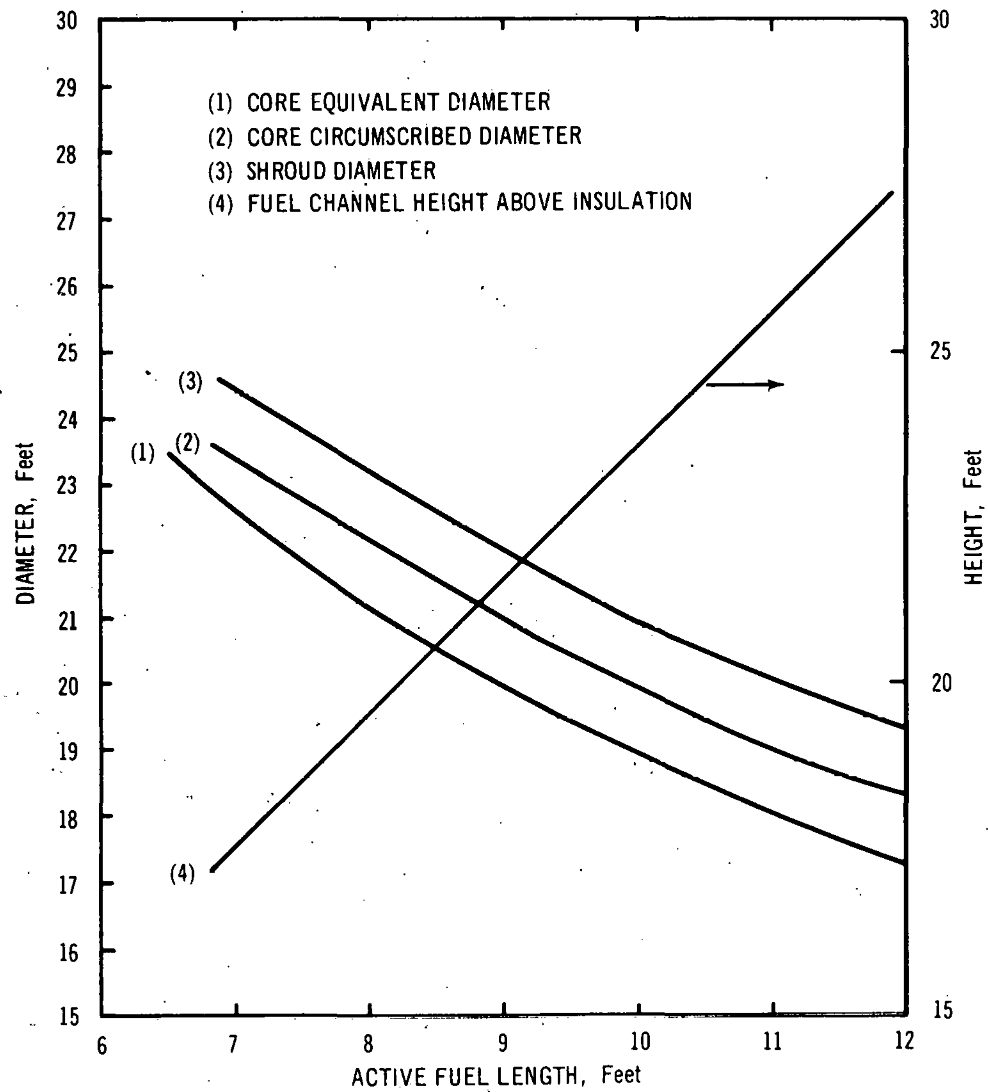

Figure 5-3. Reactor Dimensions vs Active Fuel Length for a Power Density of 40 kW/l

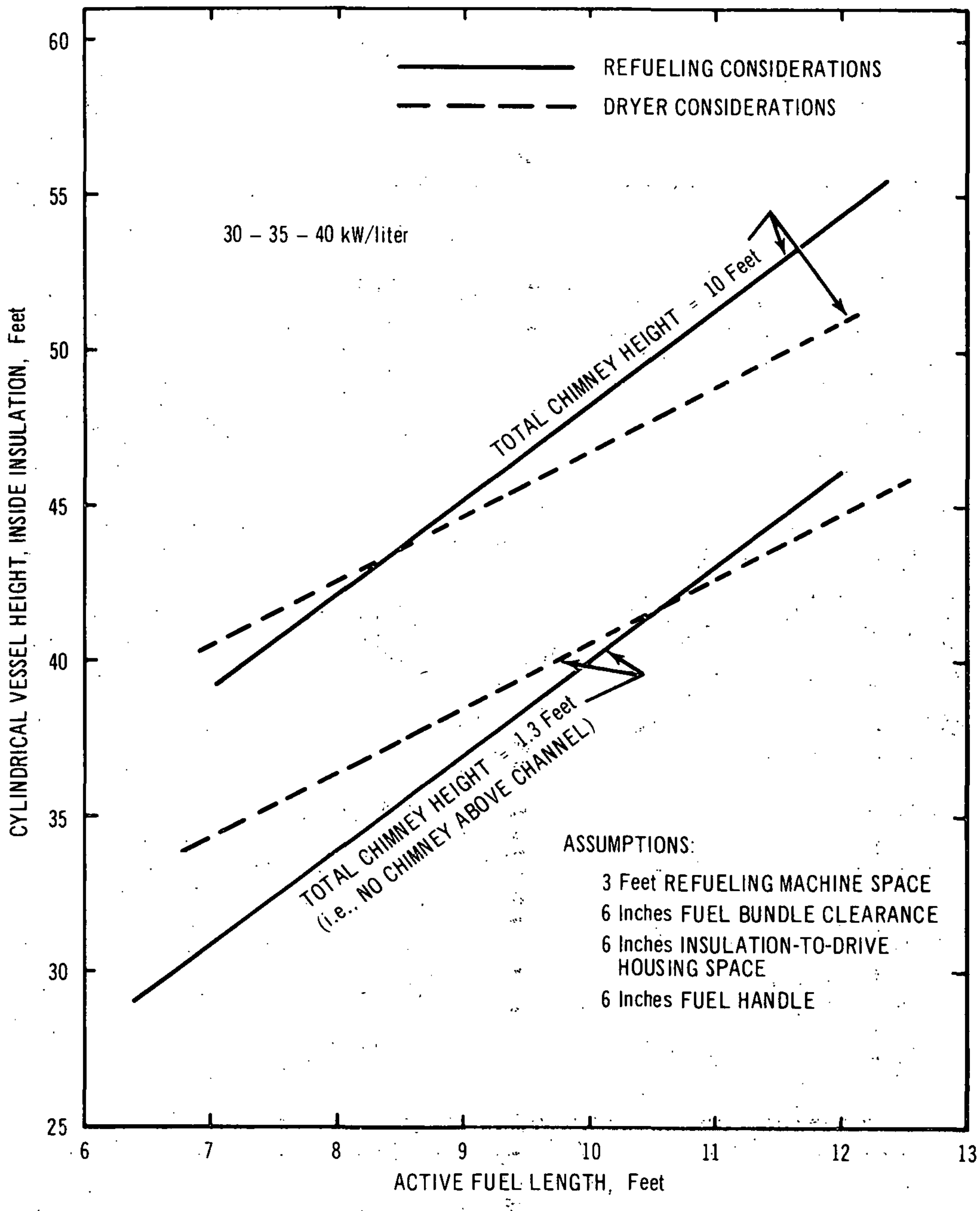

Figure 5-4. Cylindrical Vessel Height vs Active Fuel Length for Free Surface Separation

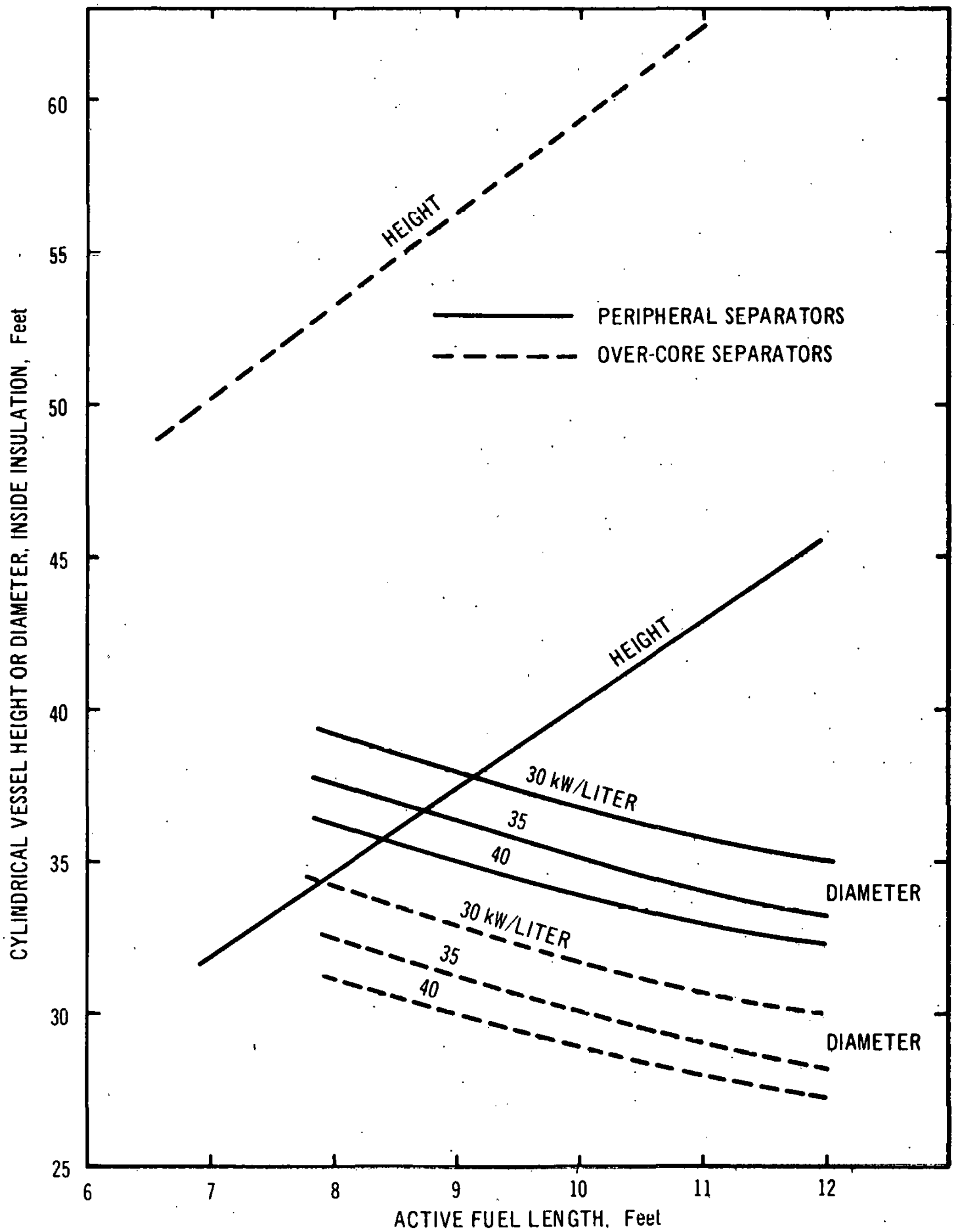

Figure 5-5. Cylindrical Vessel Height and Diameter vs Active Fuel Length for Mechanical Steam Separation

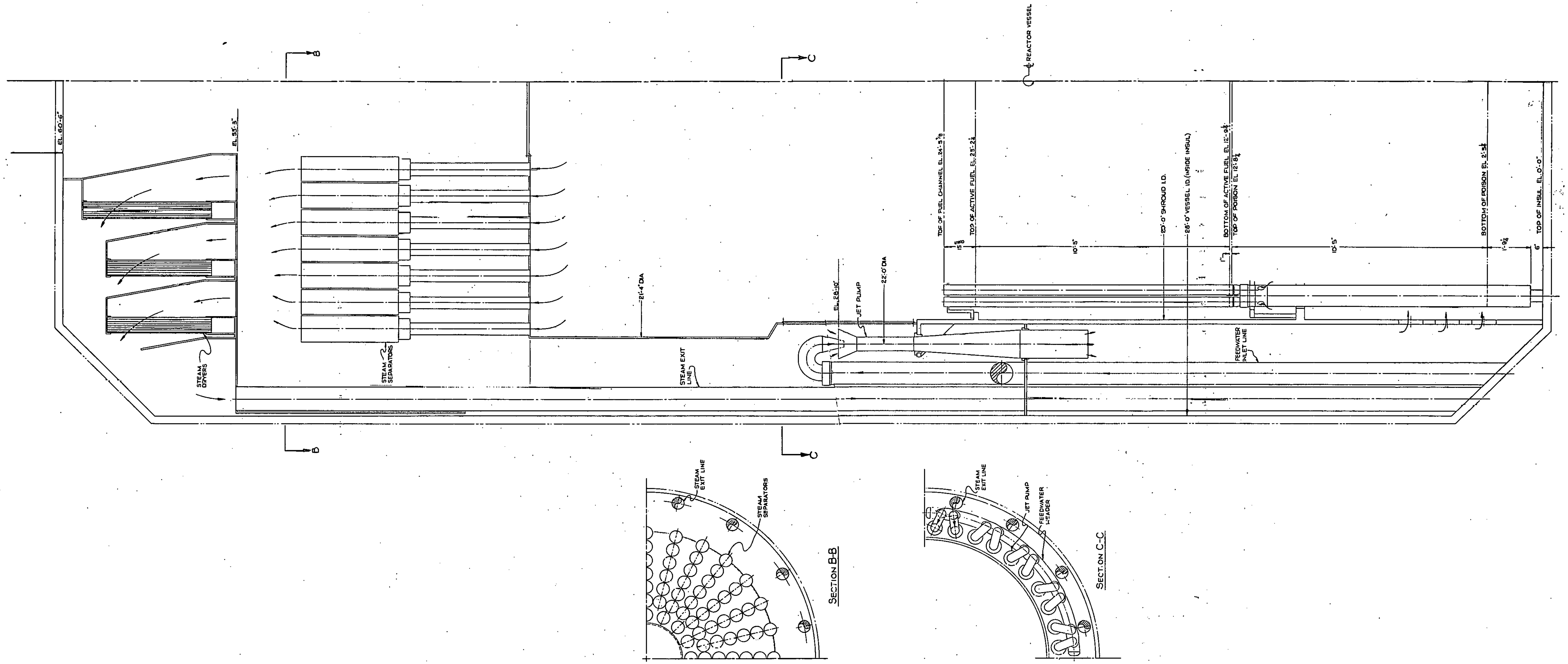

Figure 5-6. Forced Circulation, Mechanical Separation, (over core separators) Cylindrical Vessel, 10 feet - 5 in. Active Fuel Length, 40 kW/l Power Density

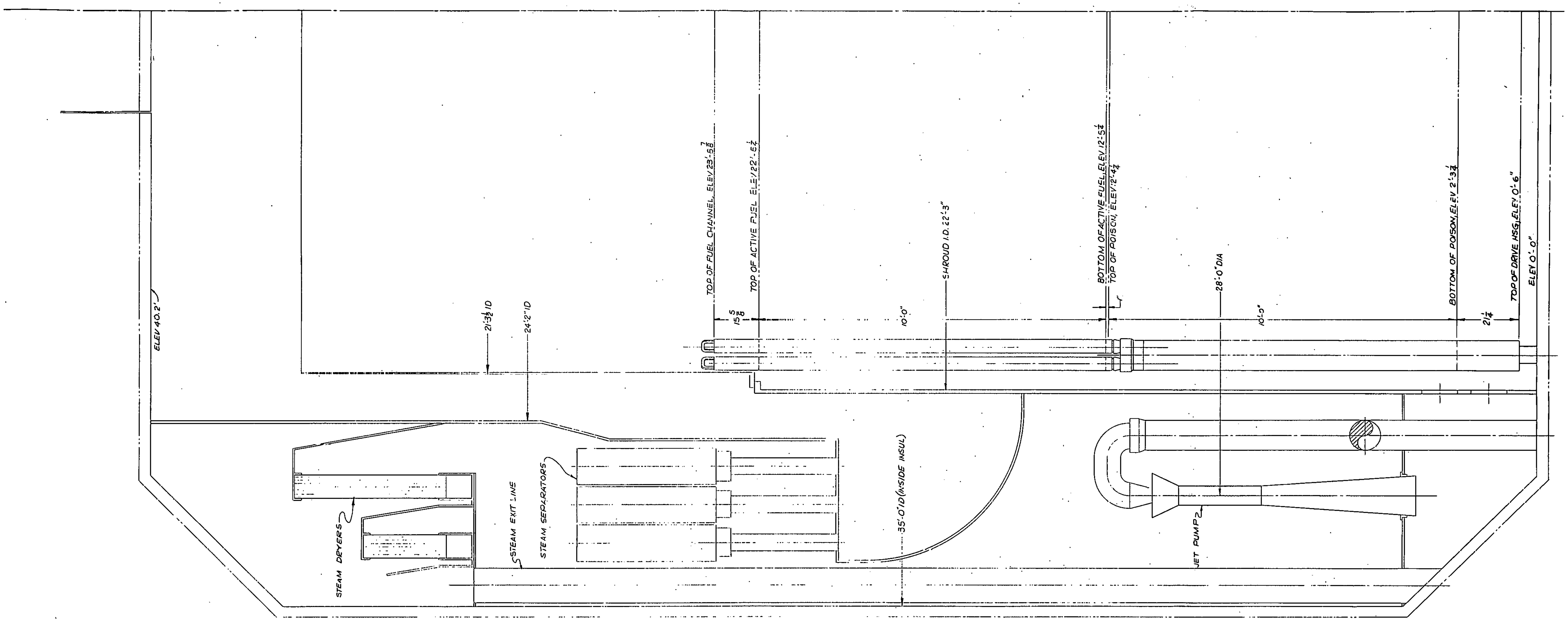

Figure 5-7. Forced Circulation, Mechanical Separation (peripheral separators) Cylindrical Vessel 10 feet-0 inch Active Fuel Length 35 kW/l Power Density

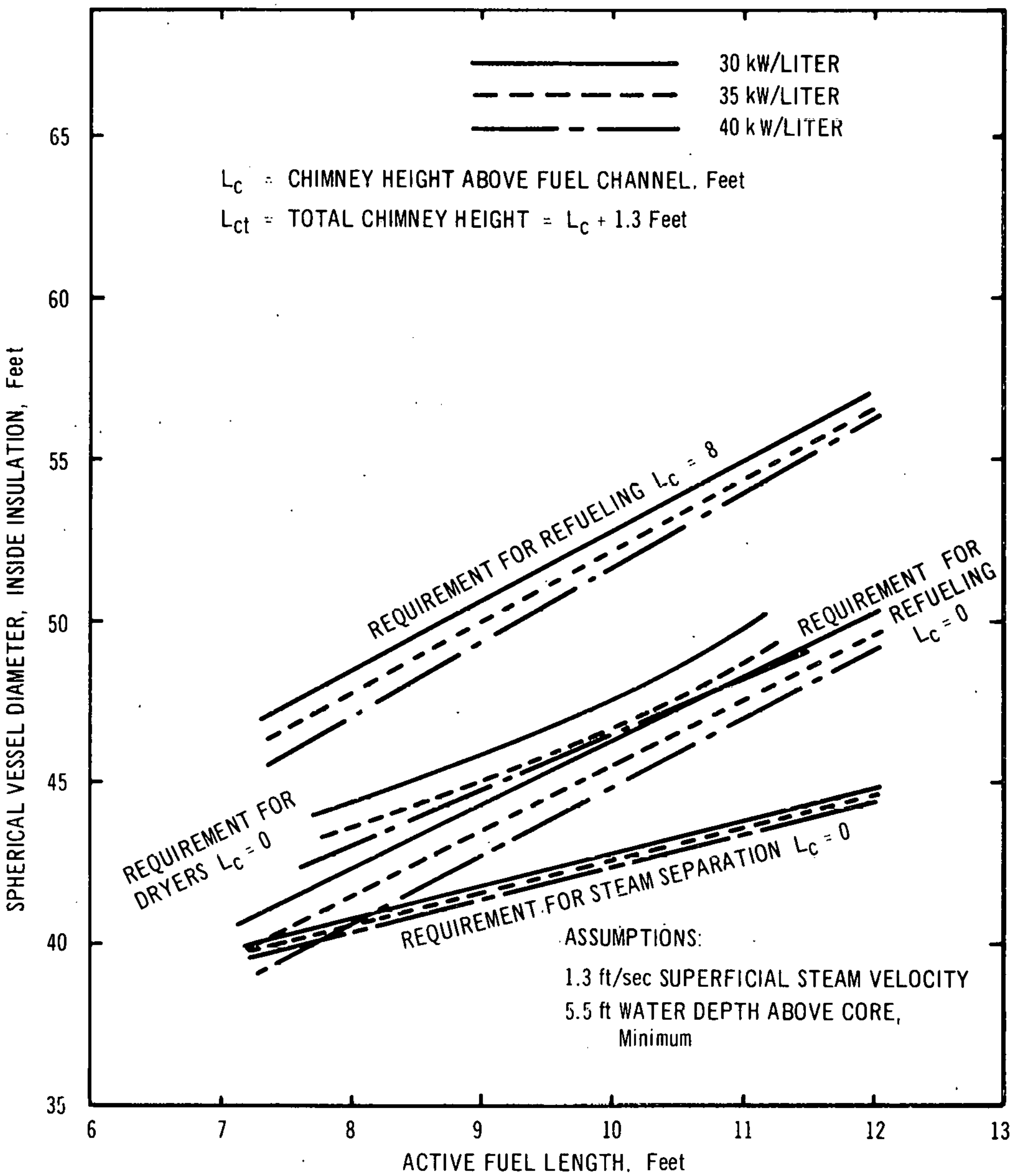

Figure 5-8. Spherical Vessel vs Active Fuel Length for Free Surface Steam Separation

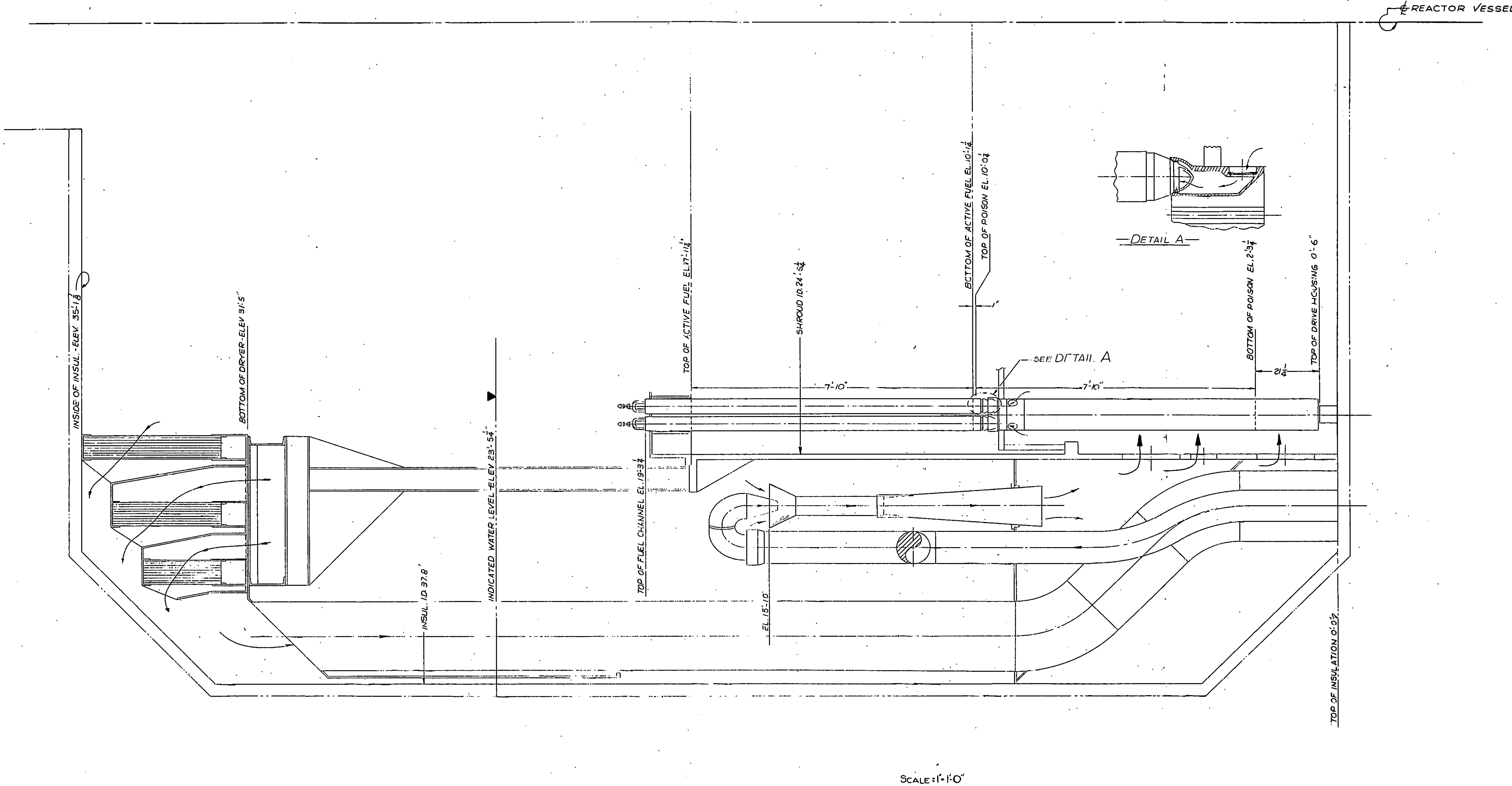

Figure 5-9. Free Surface Separation, Forced Circulation, Cylindrical Vessel, 7-ft. 10-in. Active Fuel Length, 35 kW/l Power Density

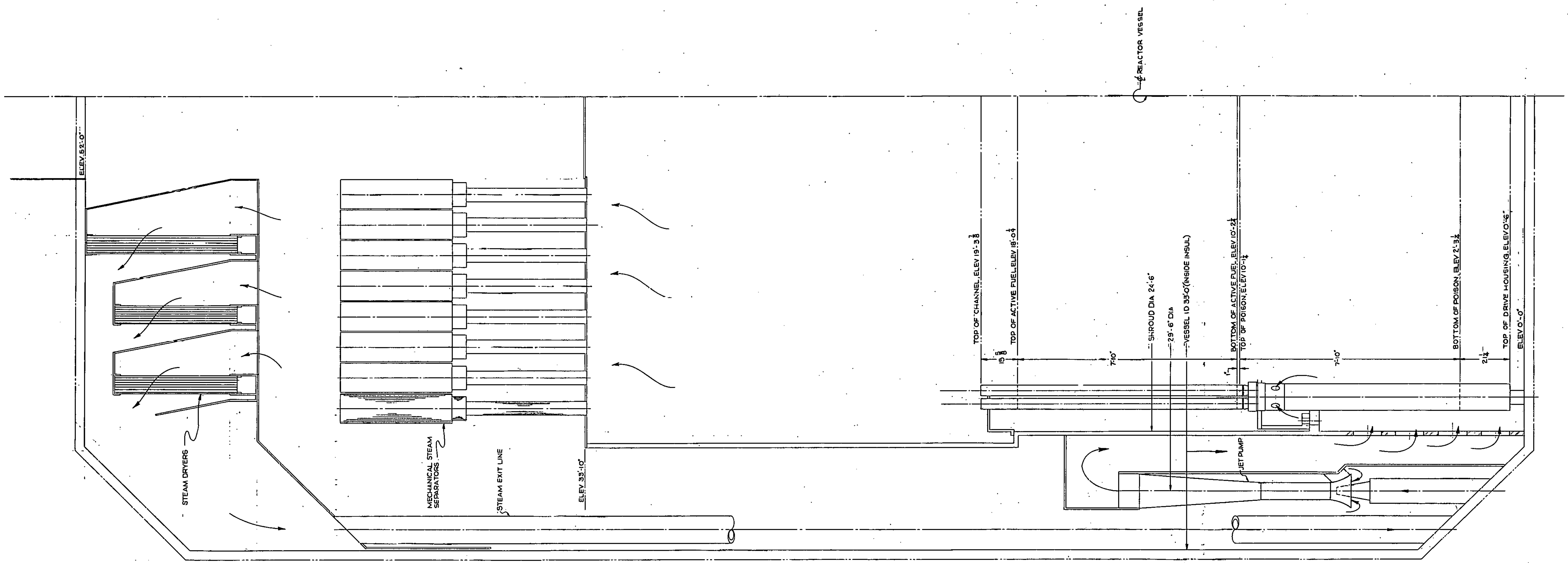

Figure 5-10. Forced Circulation, Mechanical Separation Cylindrical Vessel, 7 feet - 10 inches Active Fuel Length (Inverted Jet Pumps)

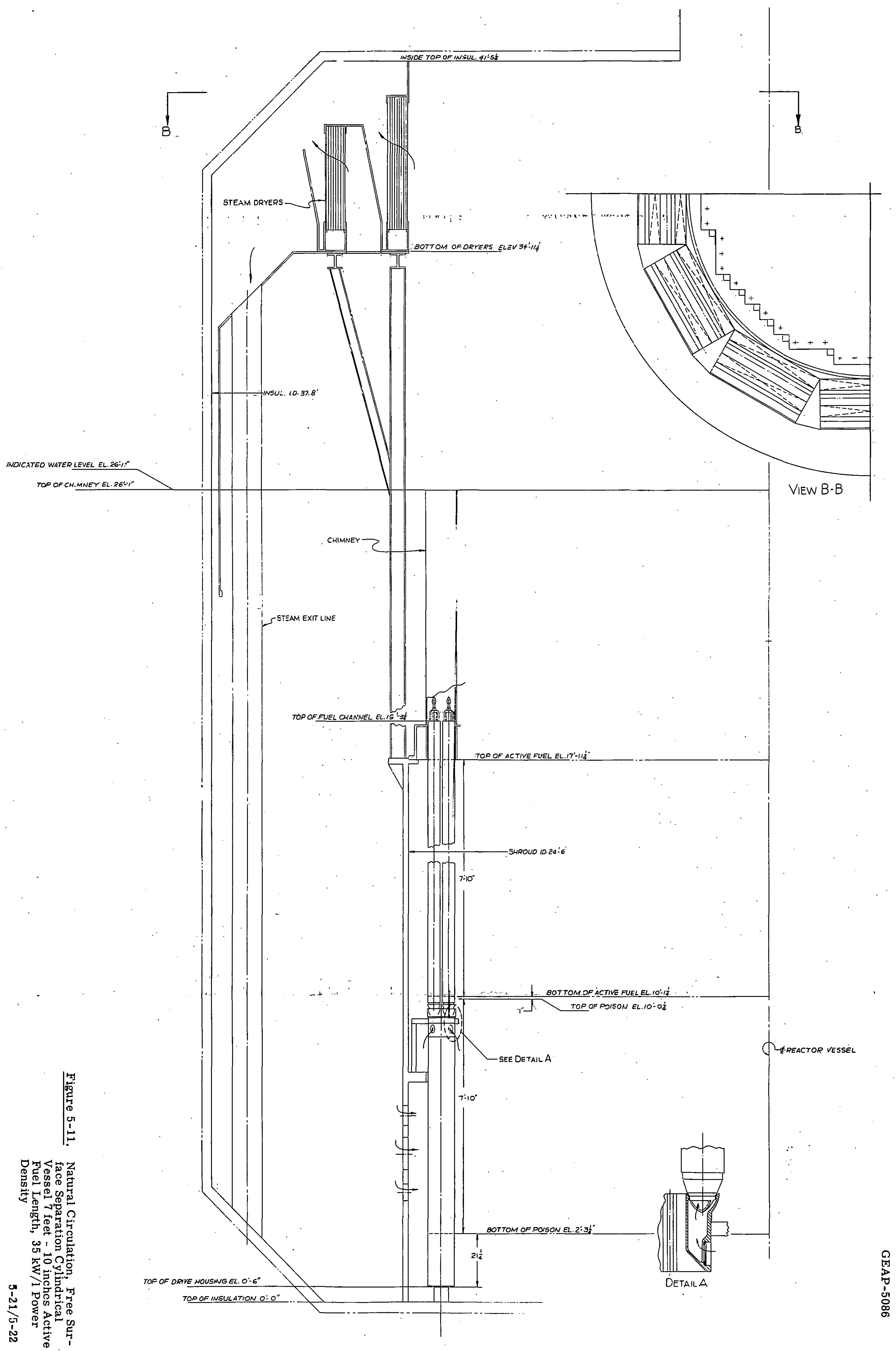

Figure 5-11. Natural Circulation, Free Surface Separation Cylindrical Vessel 7 feet - 10 inches Active Fuel Length, 35 kW/l Power Density

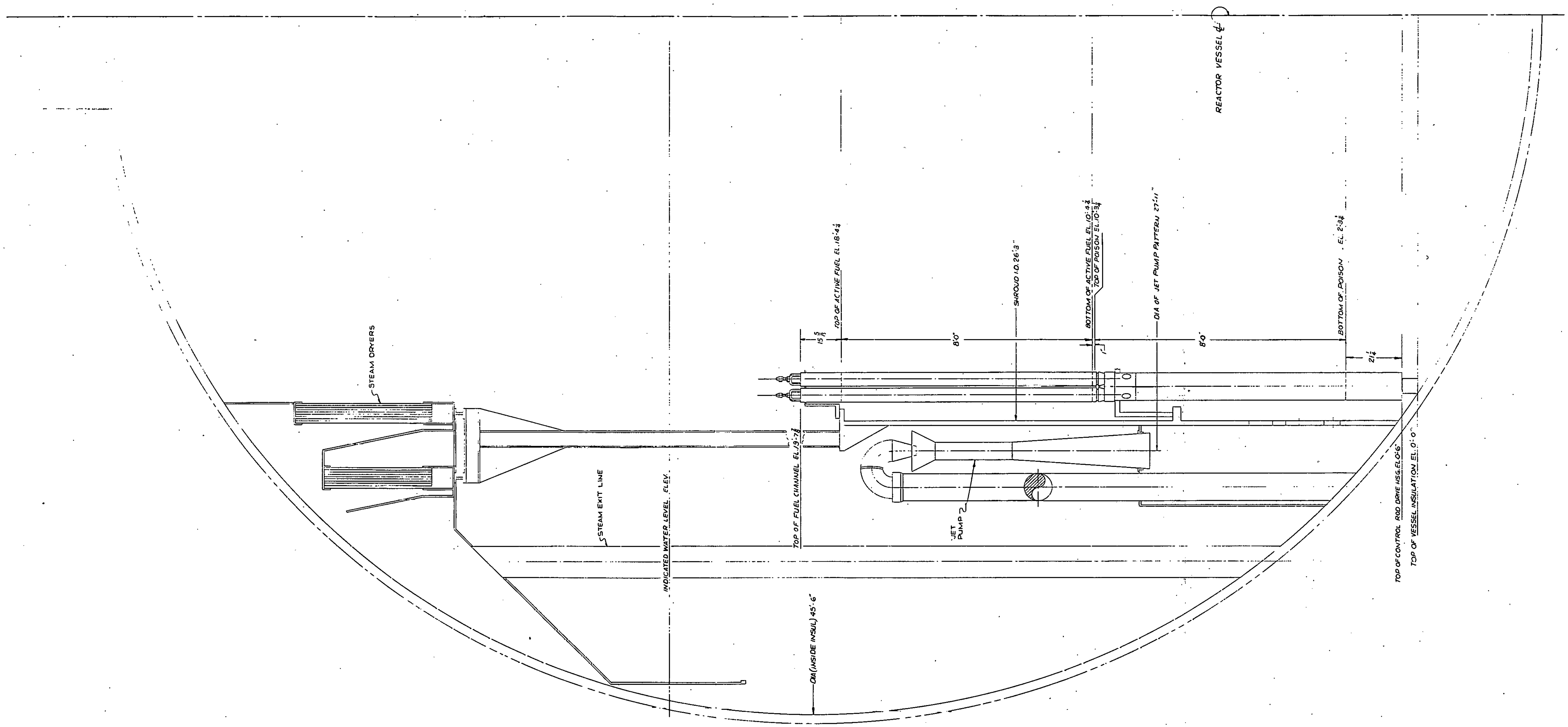

Figure 5-12. Forced Circulation, Free Surface Separation, Spherical Vessel, 8 feet - 0 inch Active Fuel Length 30 kW/l Power Density

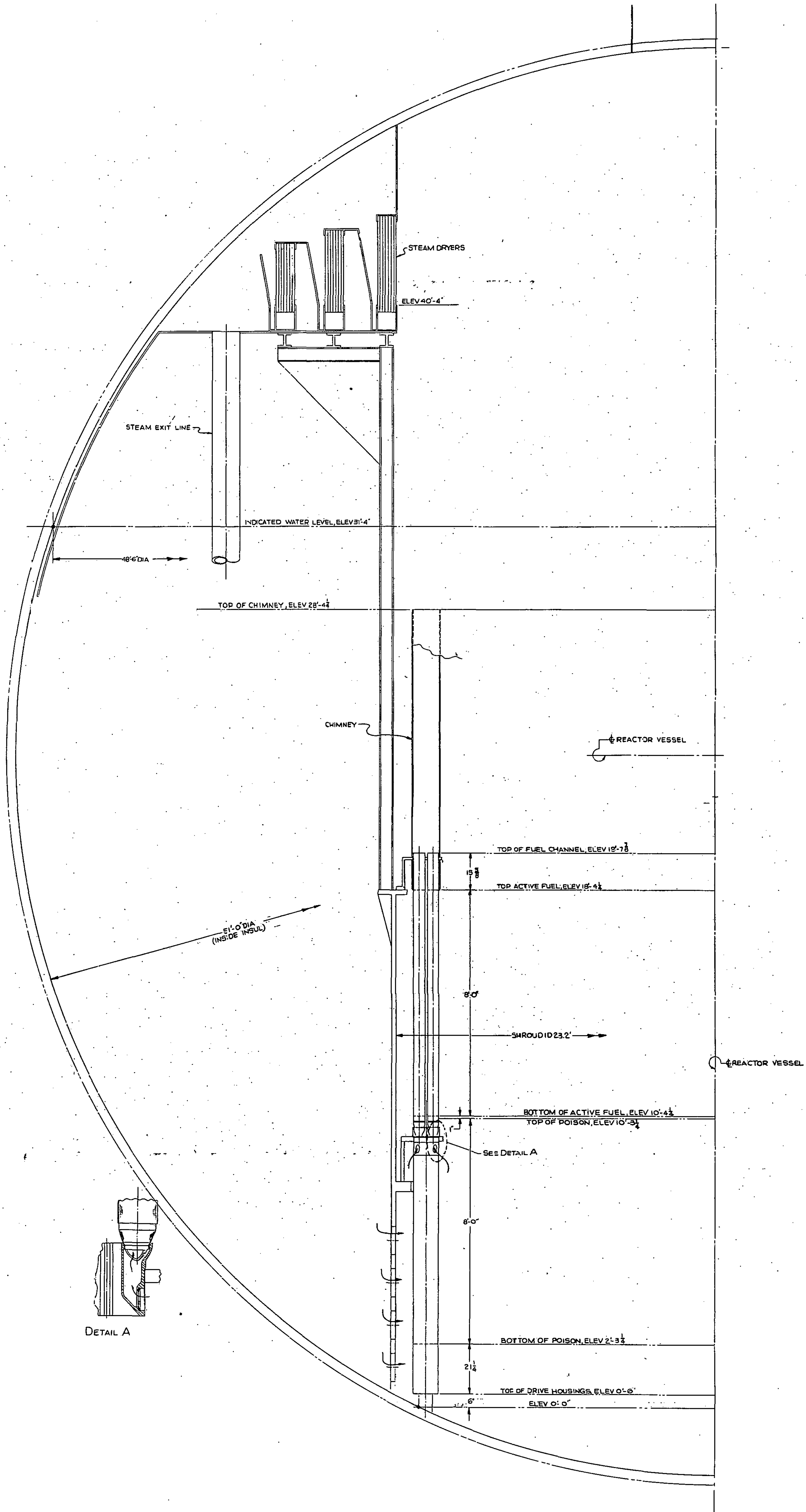

Figure 5-13. Natural Circulation Spherical Vessel 8 feet - 0 inch Active Fuel Length, 40 kW/l Power Density

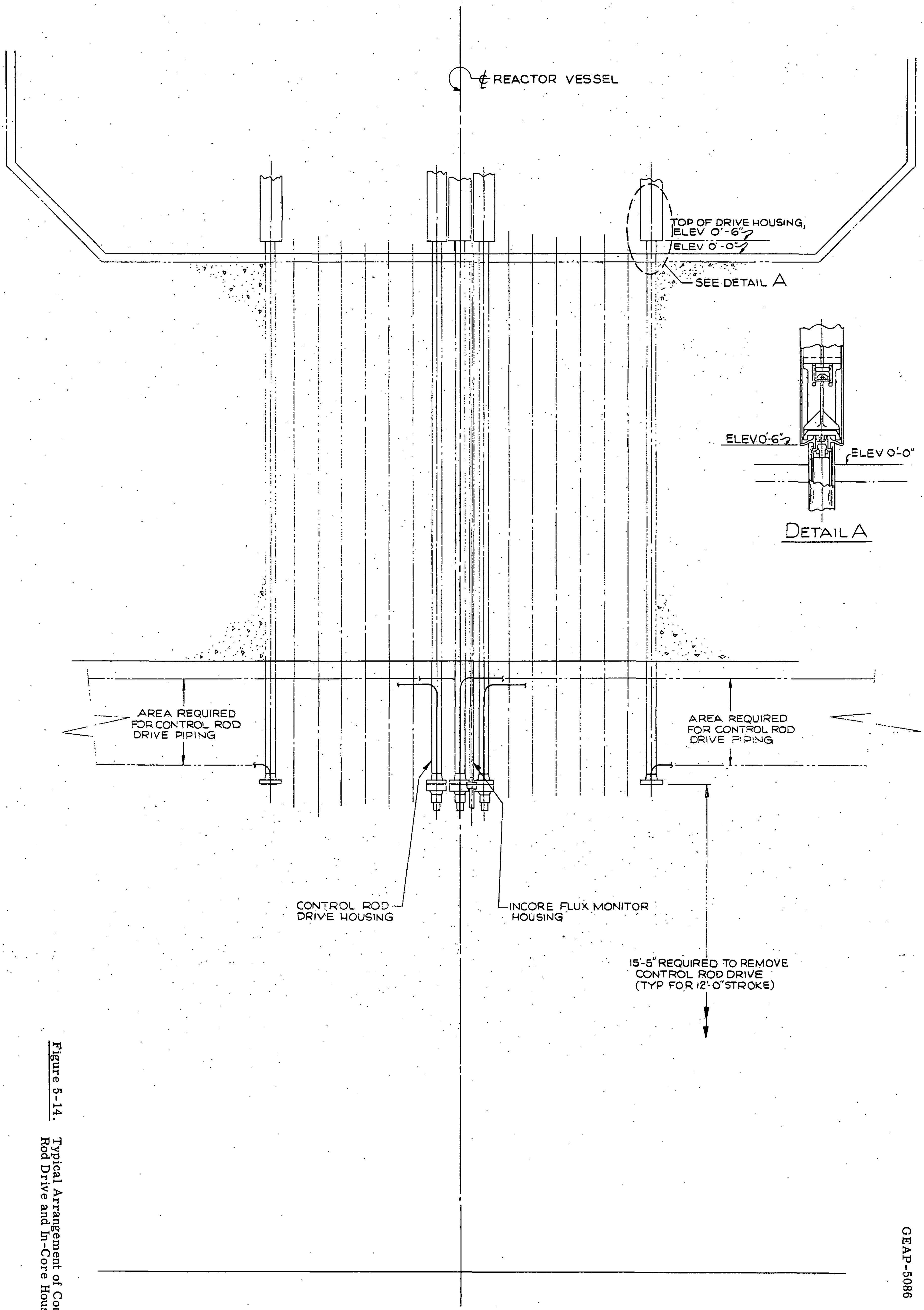

Figure 5-14. Typical Arrangement of Control Rod Drive and In-Core Housings.

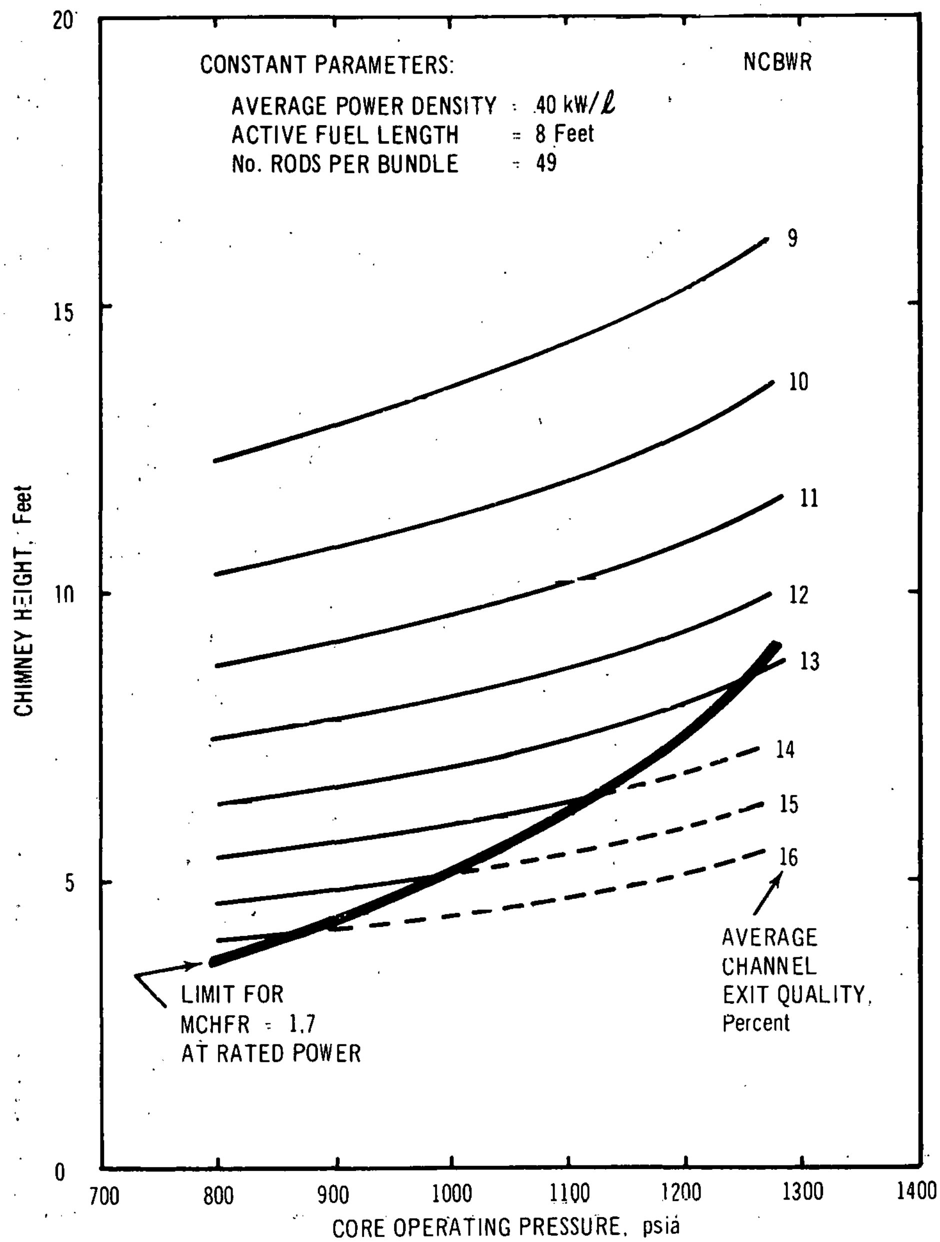

Figure 5-15. Chimney Height vs Core Pressure and Channel Exit Quality

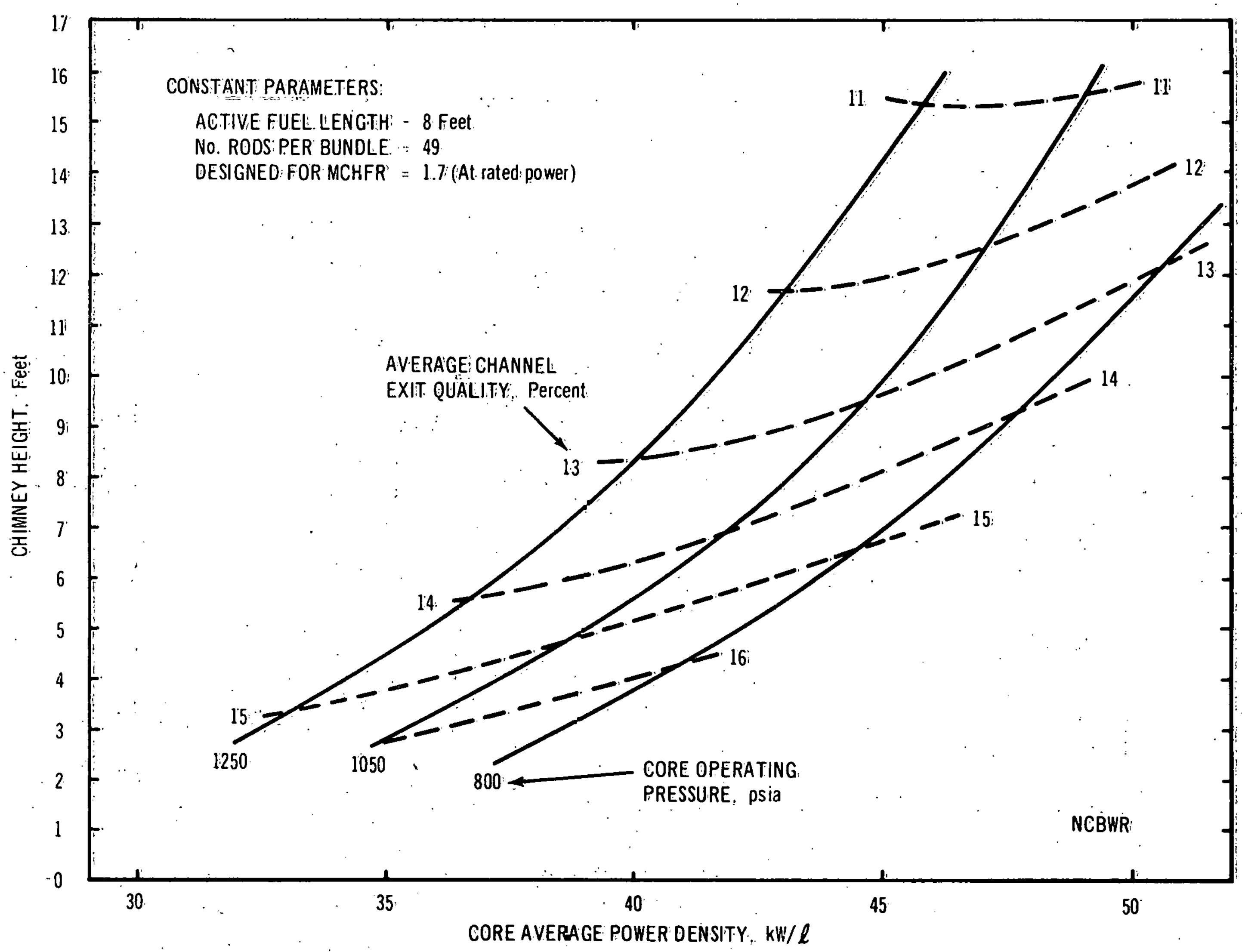

Figure 5-16. Chimney Height vs Power Density, Core Pressure and Channel Exit Quality

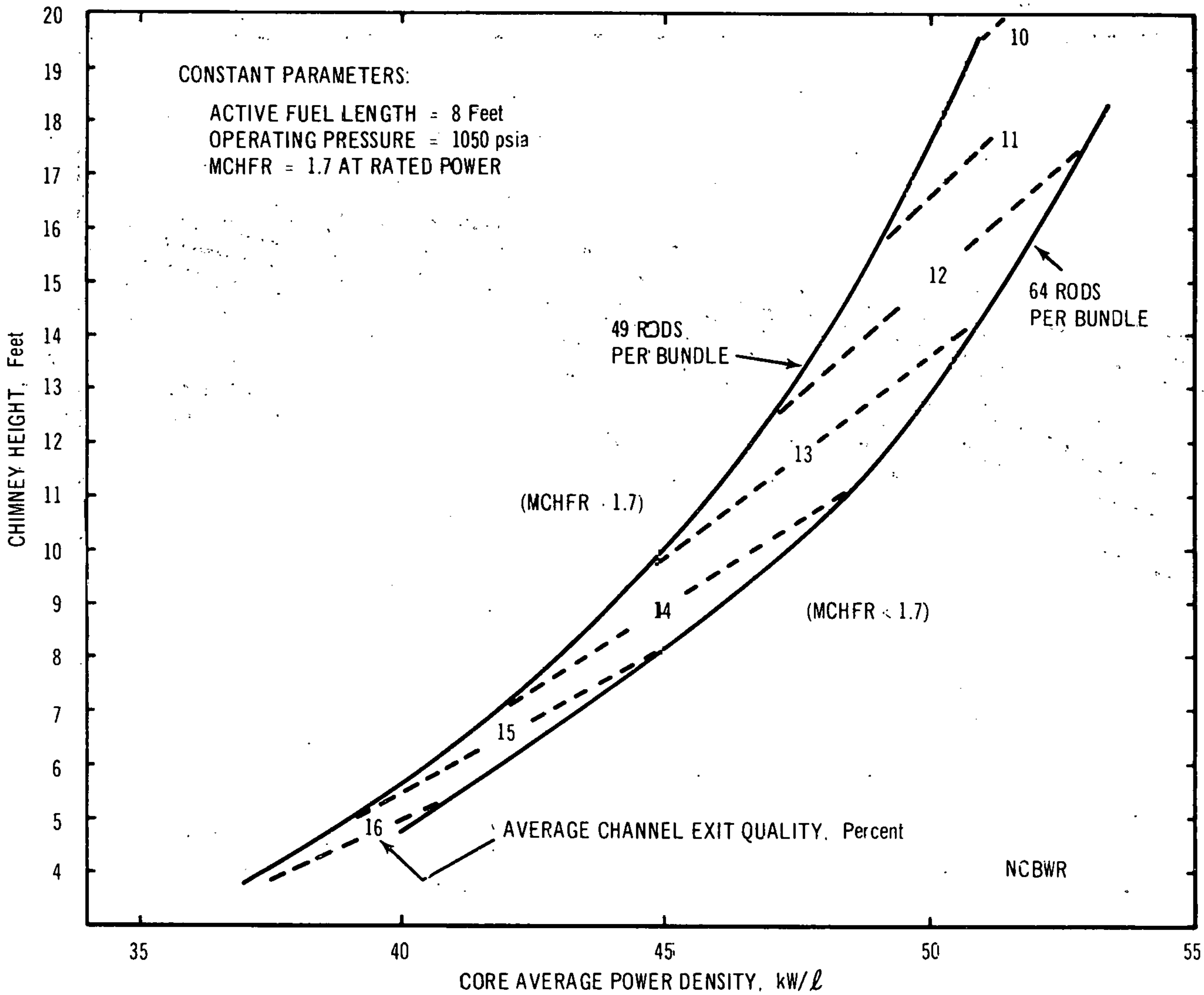

Figure 5-17. Chimney Height vs Power Density, Number of Rods per Bundle and Channel Exit Quality

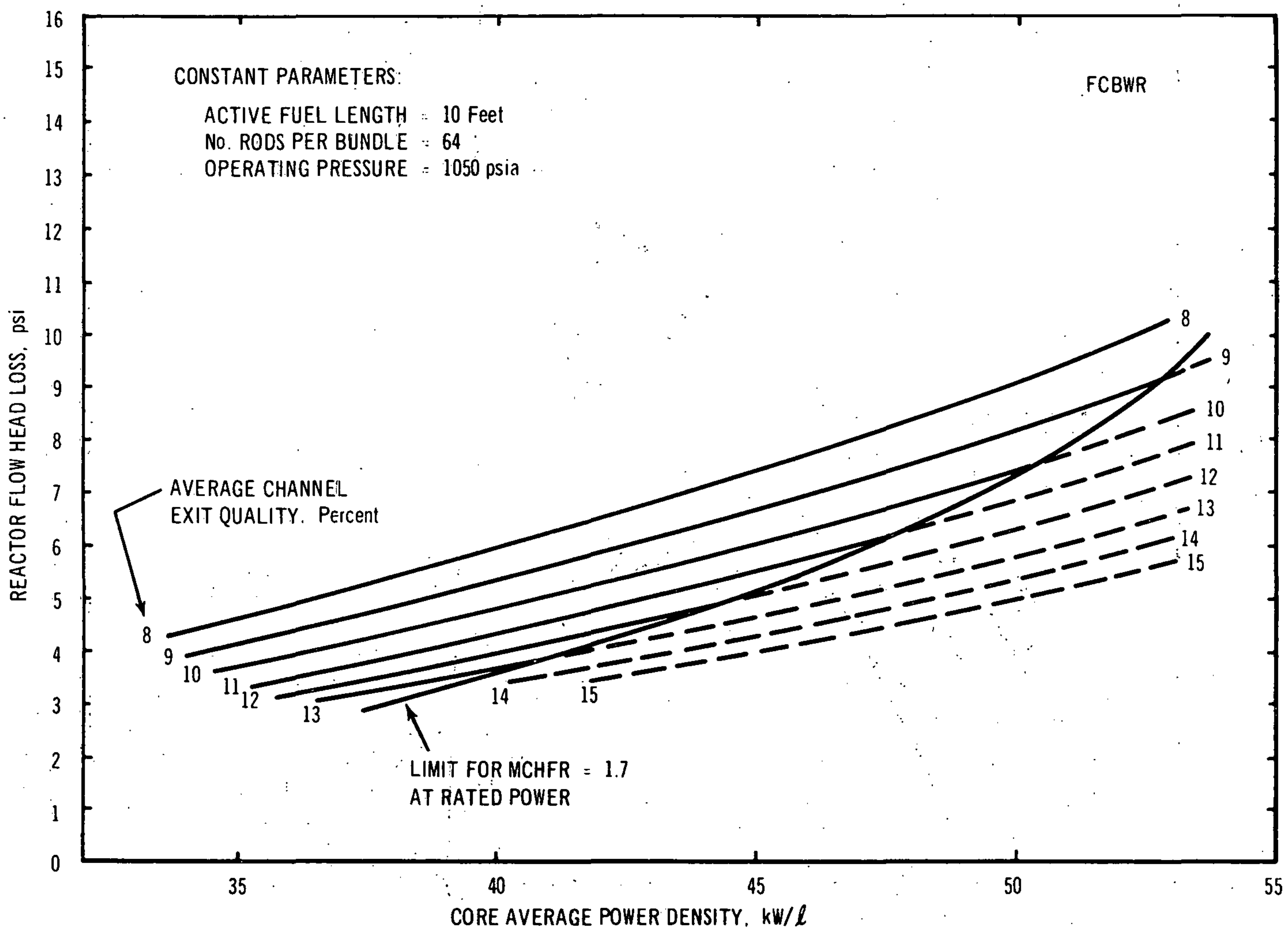

Figure 5-18. Reactor Flow Head Loss vs Power Density and Steam Exit Quality

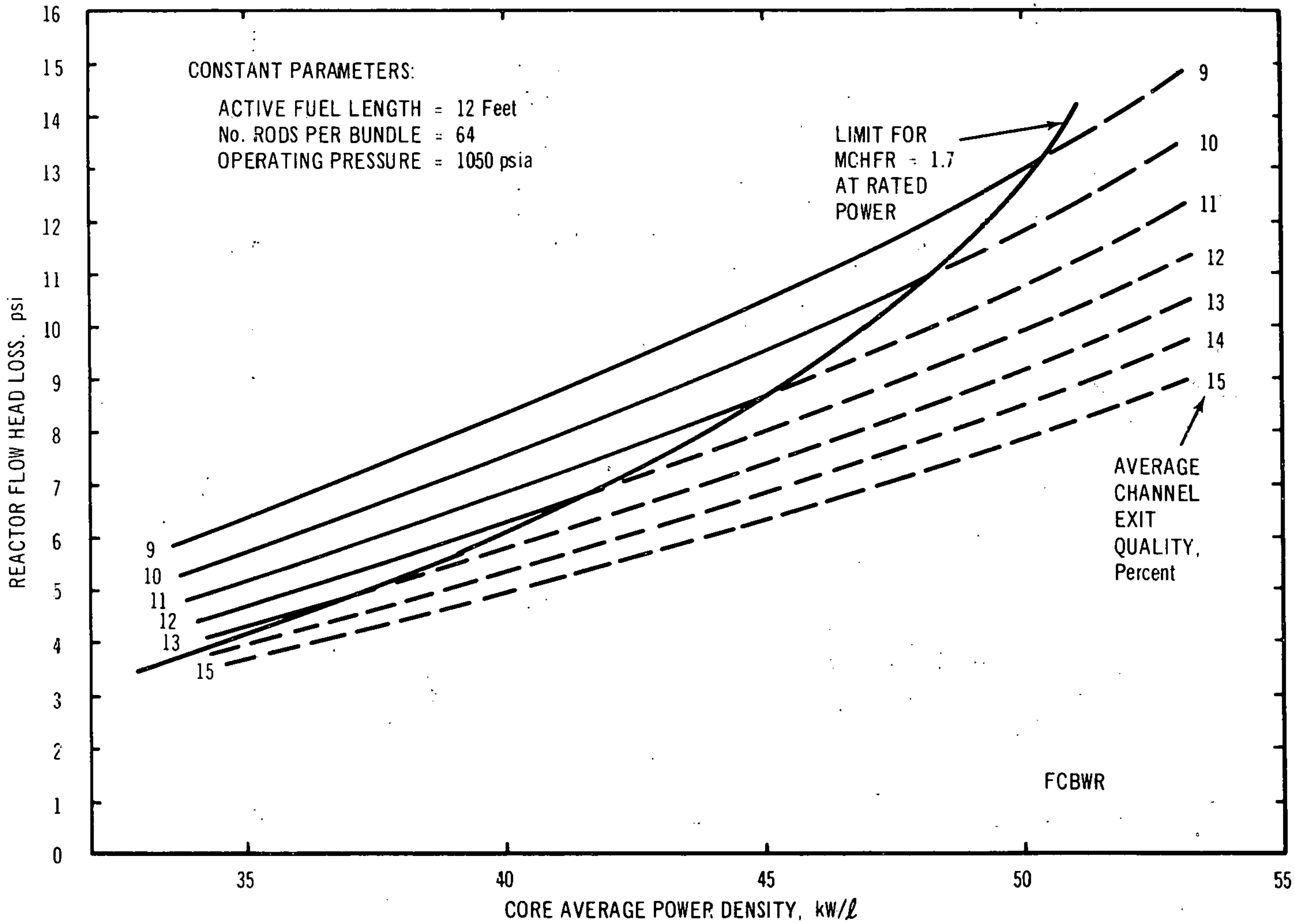

Figure 5-19. Reactor Flow Head Loss vs Power Density and Steam Exit Quality

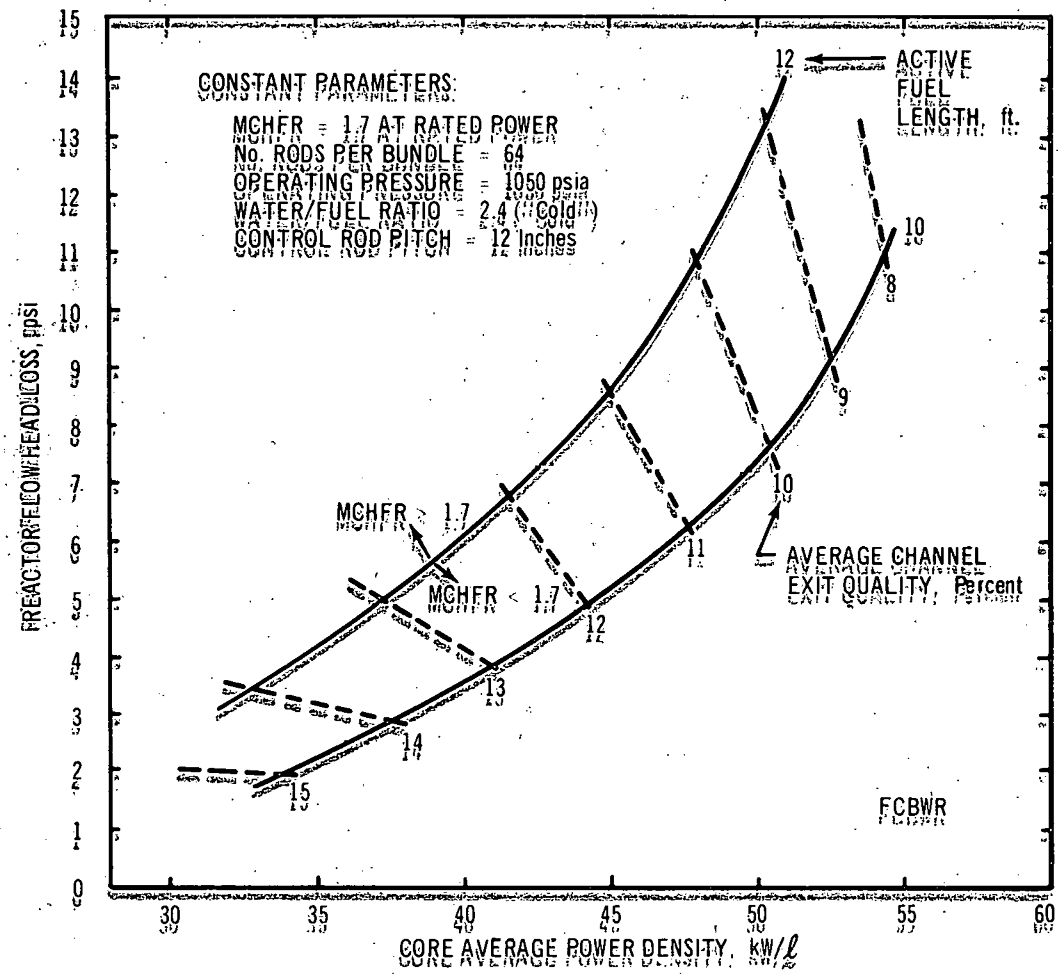

Figure 5-20. Reactor Flow Head Loss vs Power Density, Active Fuel Length and Steam Exit Quality

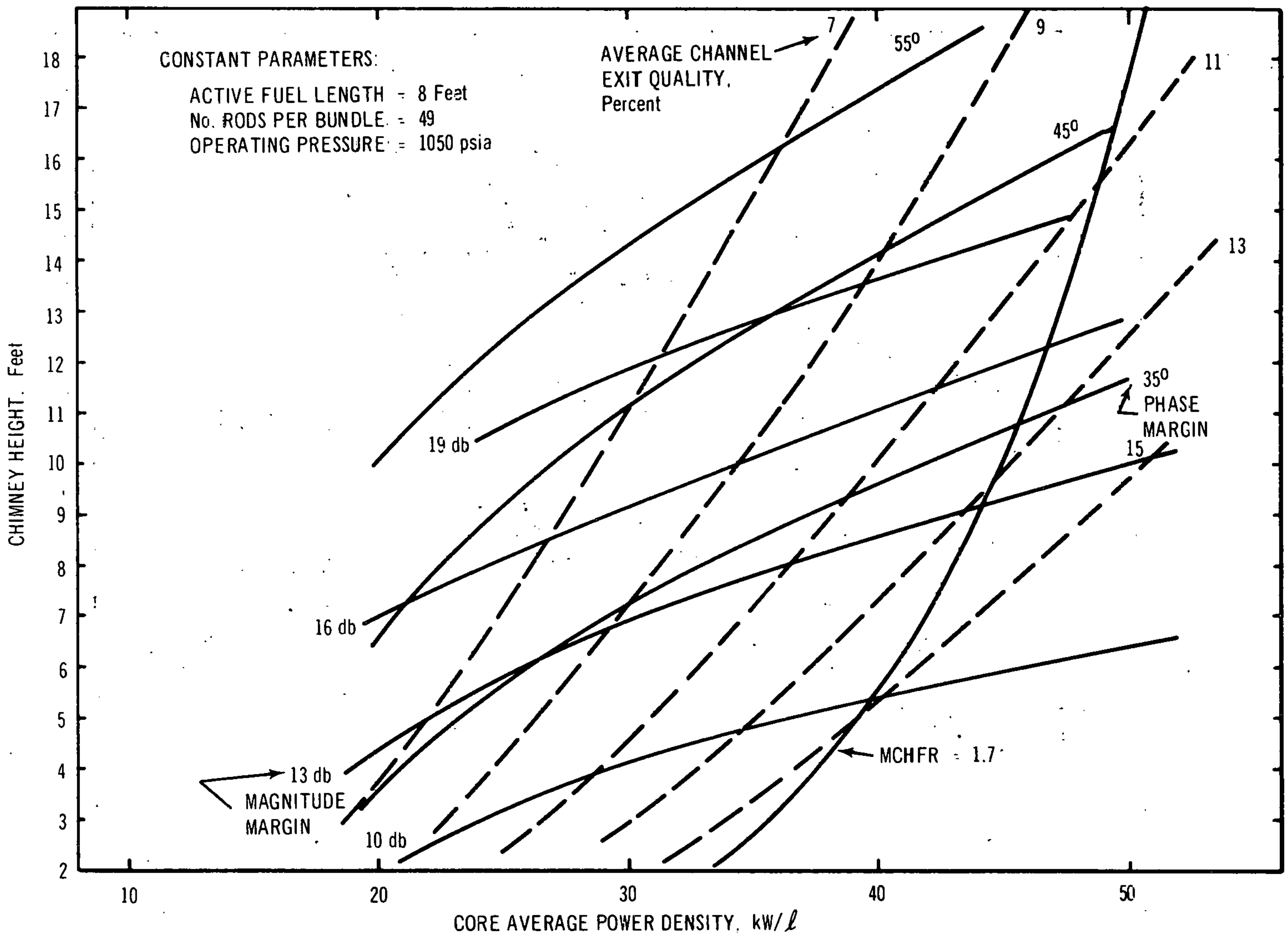

Figure 5-21. Isophase and Isomagnitude Margin Curves

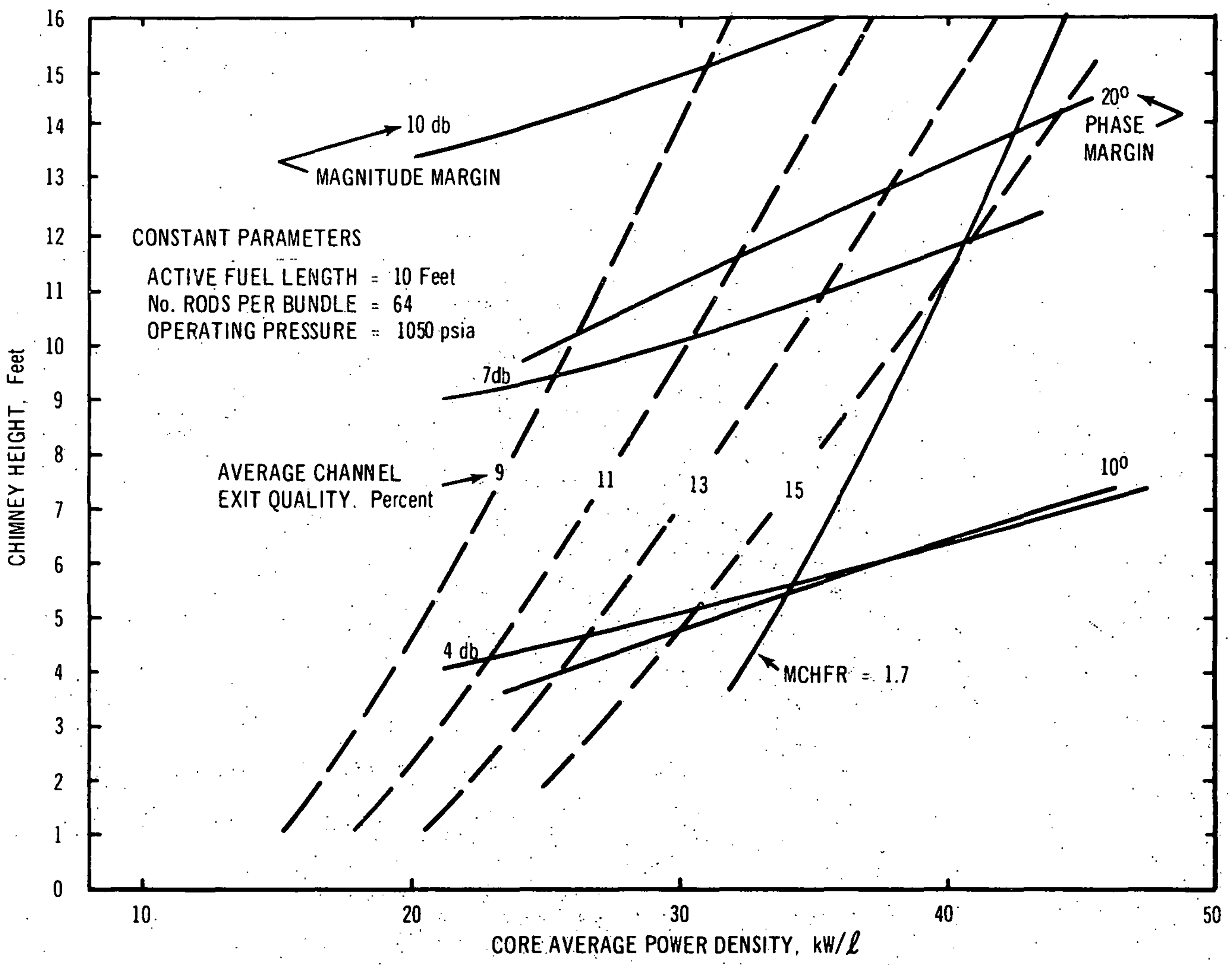

<u>Figure 5-22.</u> Isophase and Isomagnitude Margins

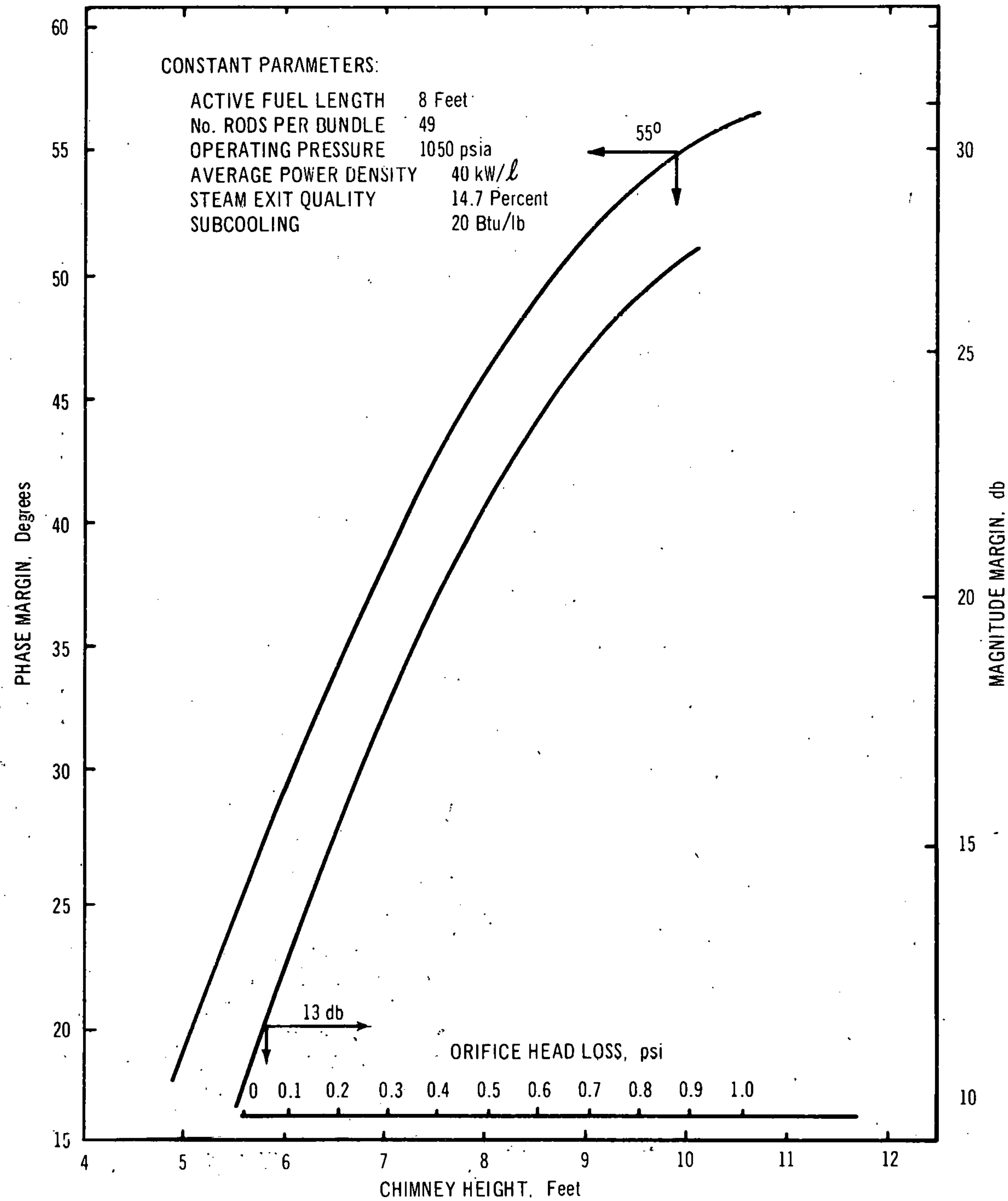

Figure 5-23. Phase and Magnitude Margins vs Chimney Height or Orifice Head Loss

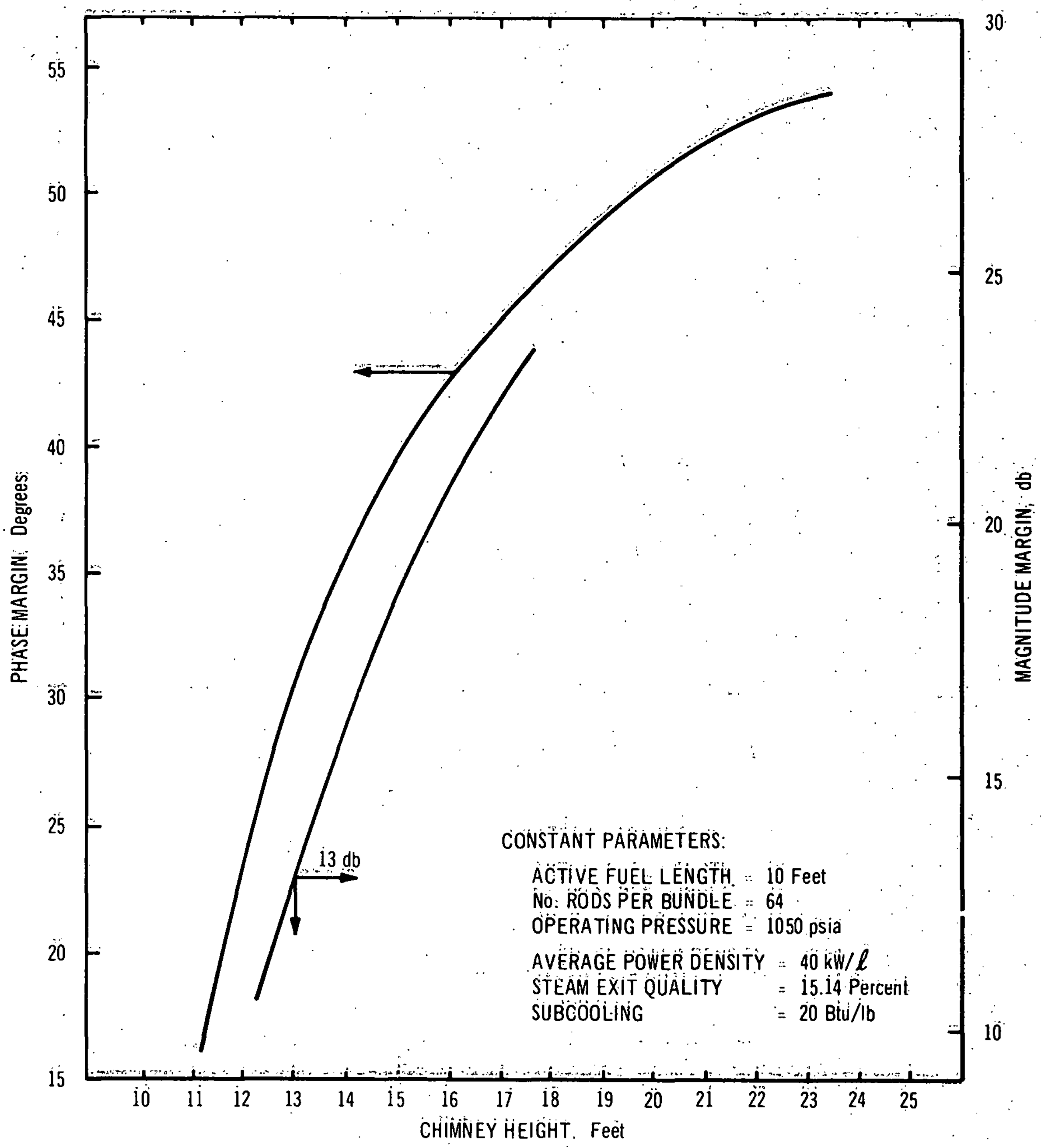

Figure 5-24. Phase and Magnitude Margins vs Chimney Height

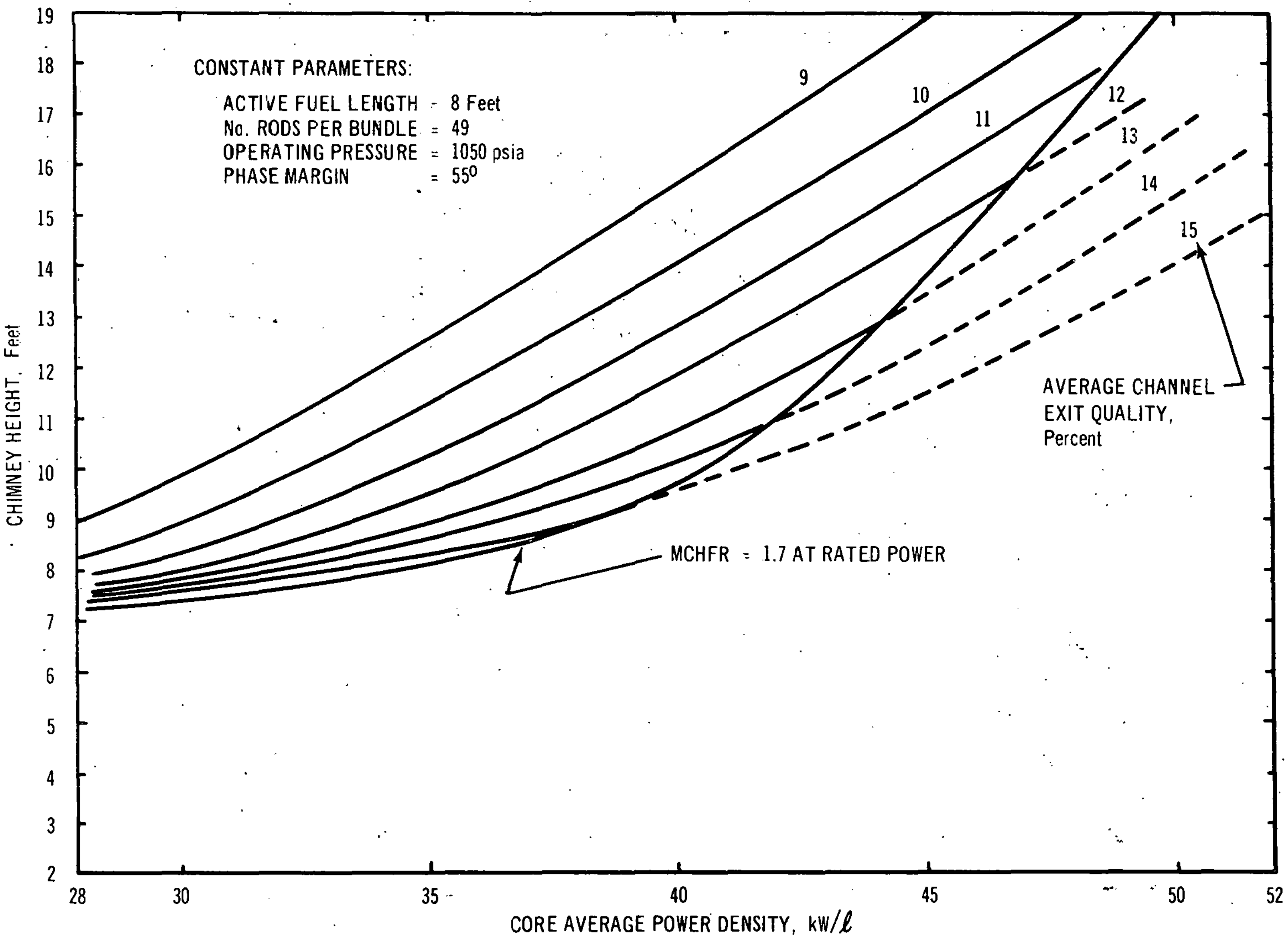

Figure 5-25. Chimney Length vs Average Power Density and Steam Exit Quality with Orificing

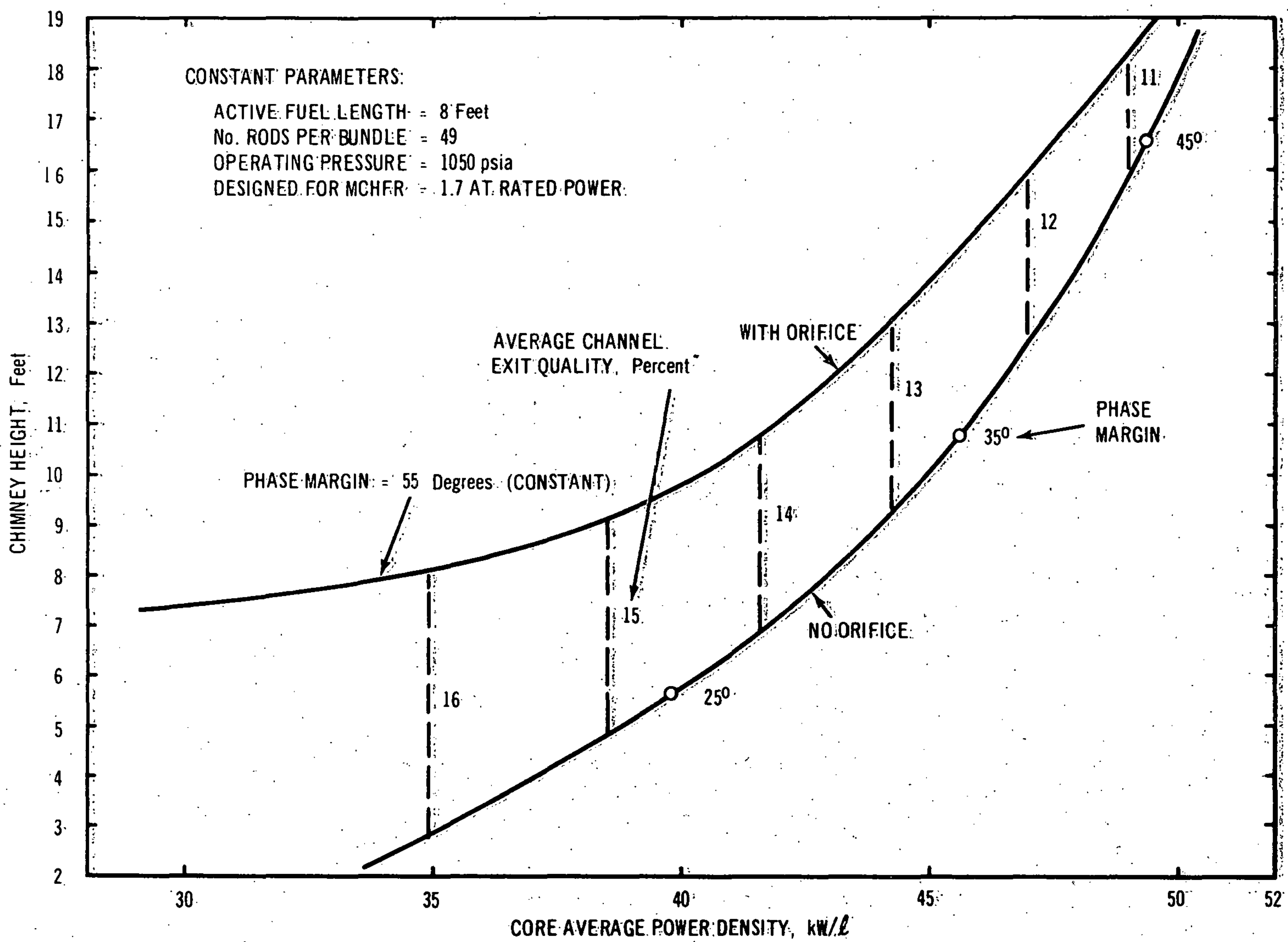

Figure 5-26. Chimney Length vs Average Power Density and Steam Exit Quality with and without Orificing

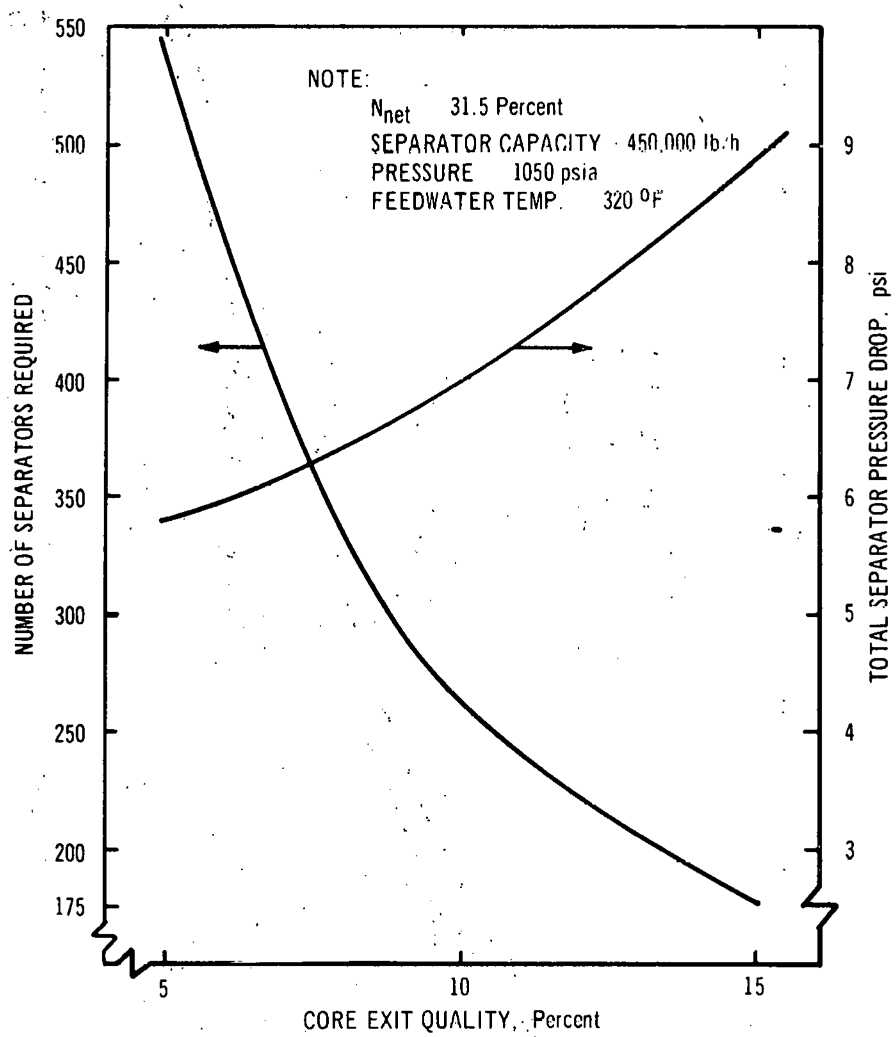

Figure 5-27. Number of Separators Required and Separator Pressure Drop vs Core Exit Quality

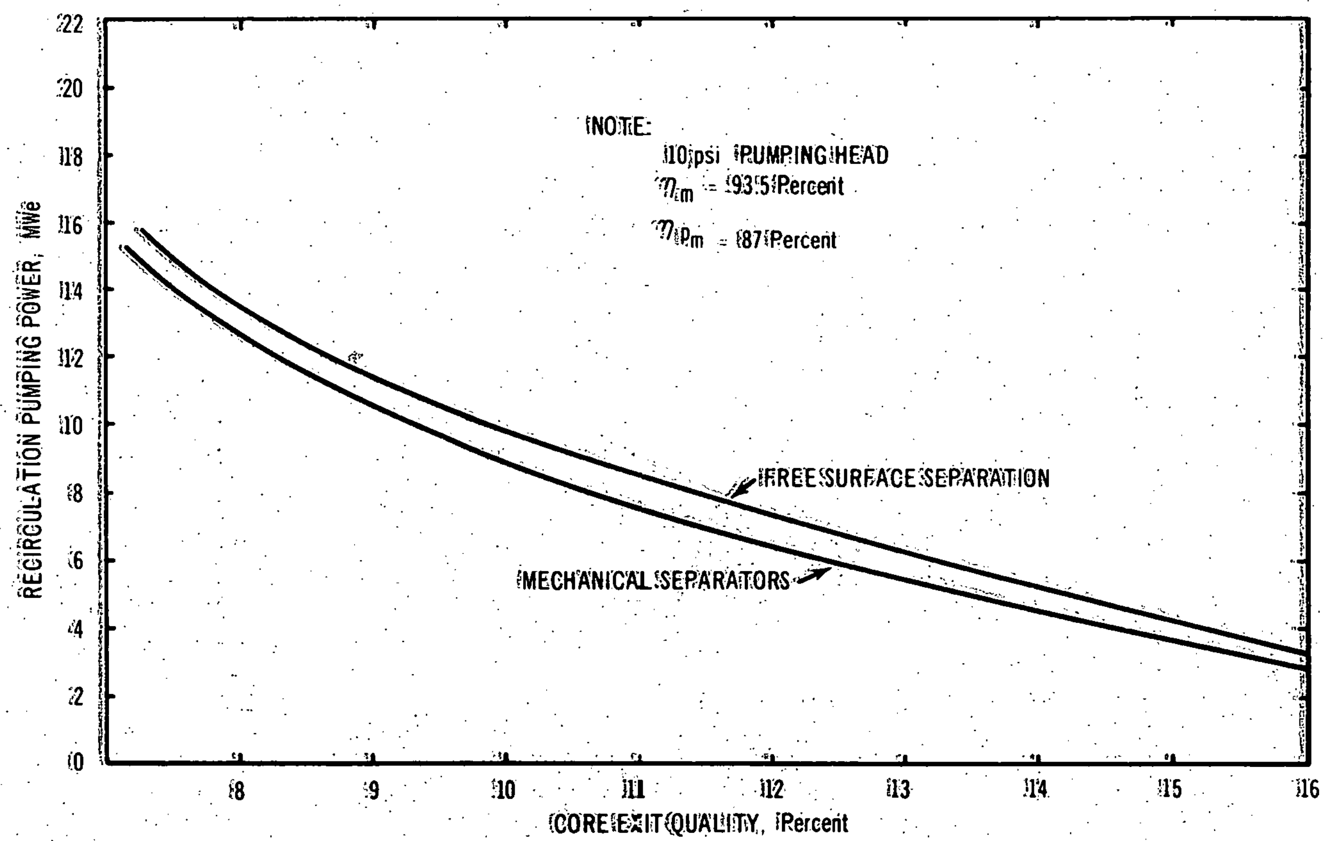

Figure 5-28. Coolant Recirculation Pumping Power vs Steam Exit Quality for Free Surface Steam Separation and Mechanical Separation Concepts (Mechanical Pumps)

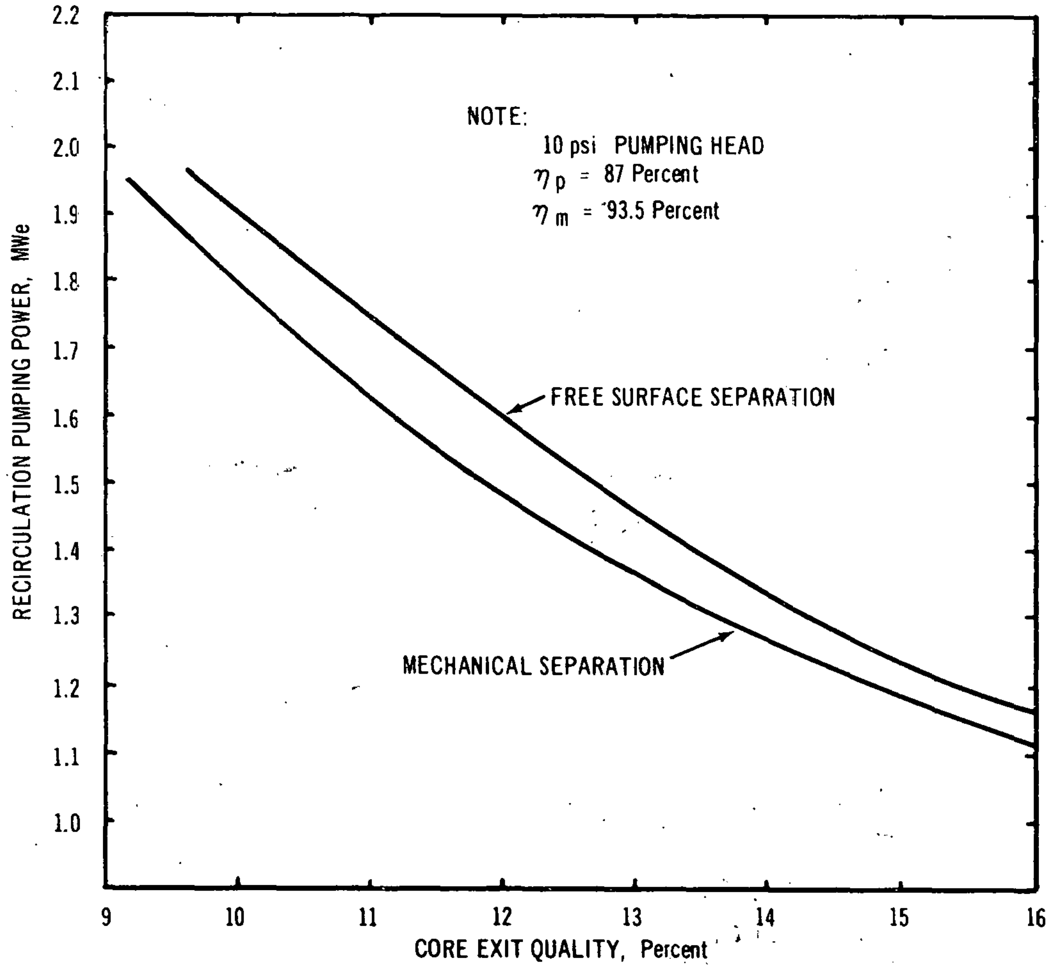

Figure 5-29. Coolant Recirculation Pumping Power vs Steam Exit Quality for Free Surface Steam Separation and Mechanical Steam Separation Concepts (Jet Pumps)

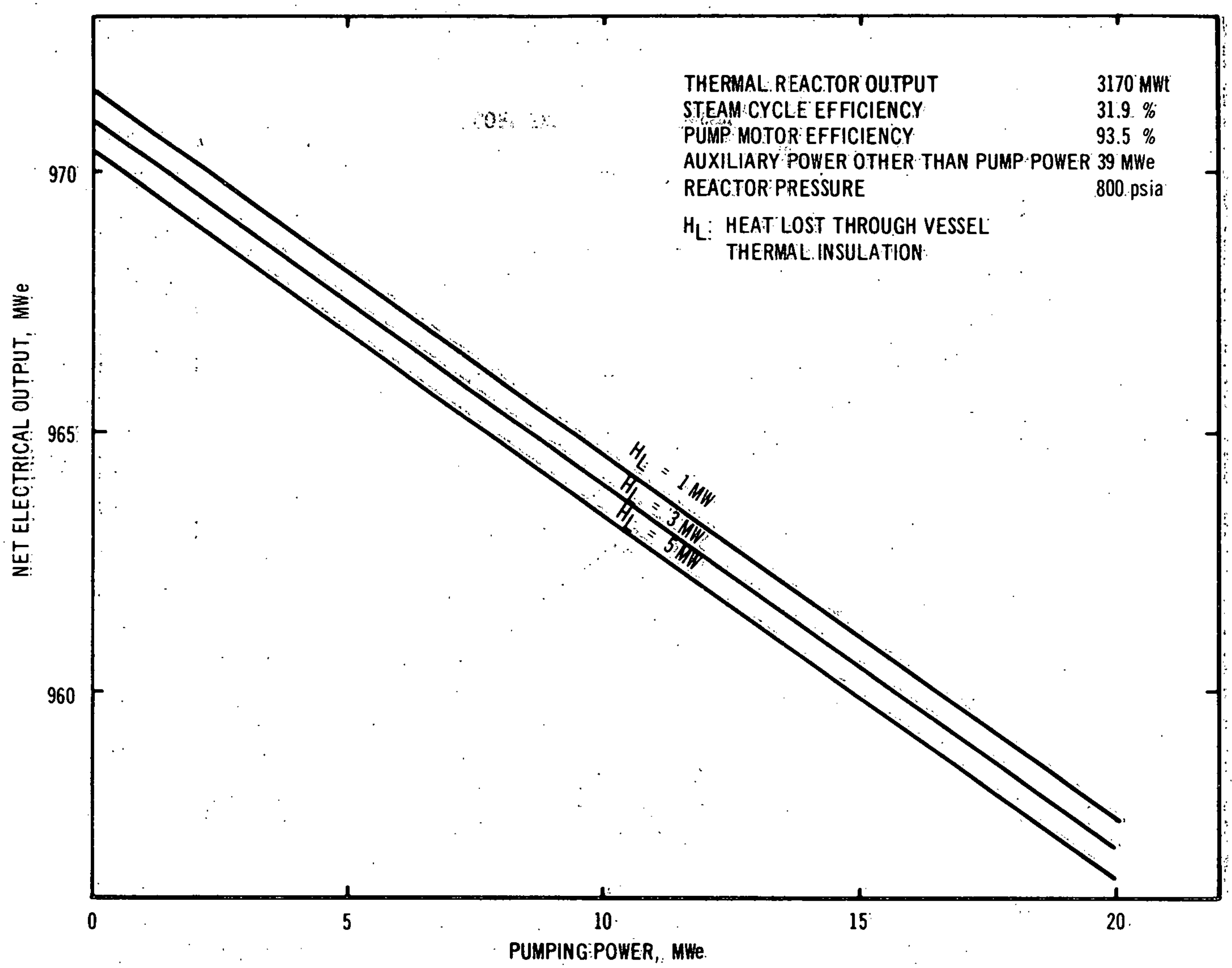

Figure 5-30. Net Electrical Output vs Pumping Power and Heat Loss Through Insulation for Reactor Pressure of 800 psia.

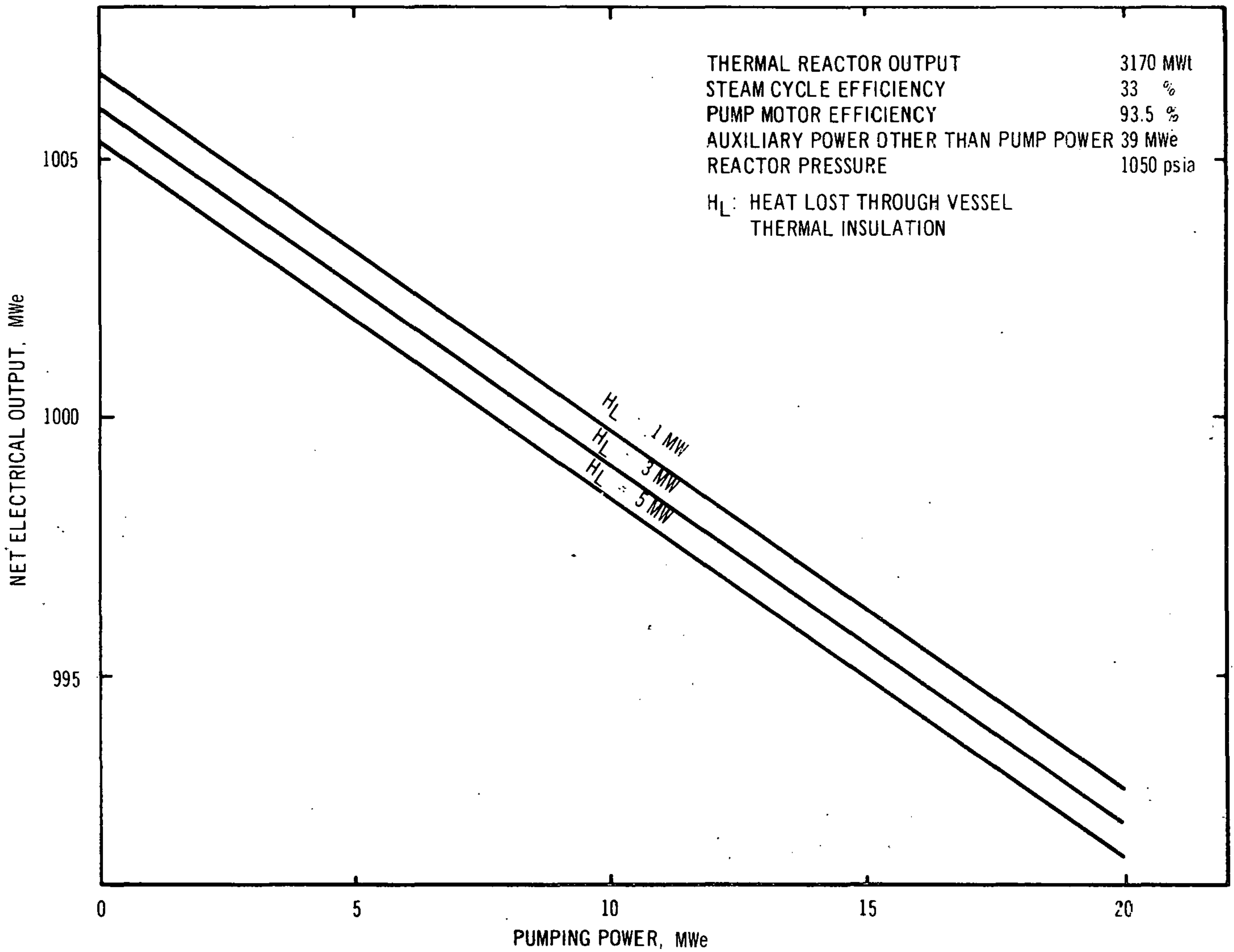

Figure 5-31. Net Electrical Output vs Pumping Power and Heat Loss through Insulation for a Reactor Pressure of 1050 psia

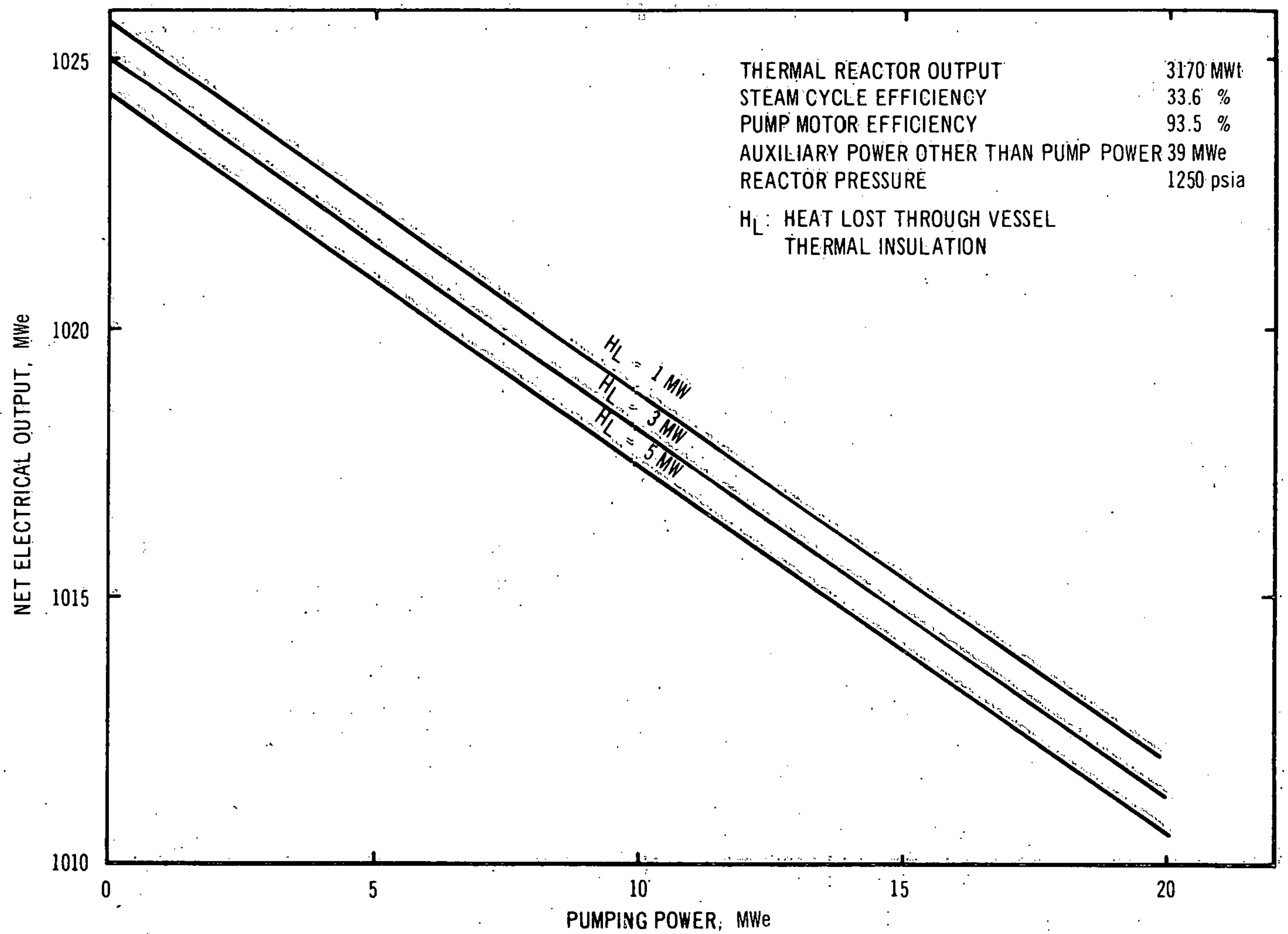

Figure 5-32. Net Electrical Output vs Pumping Power and Heat Loss through Insulation for a Reactor Pressure of 1250 psia

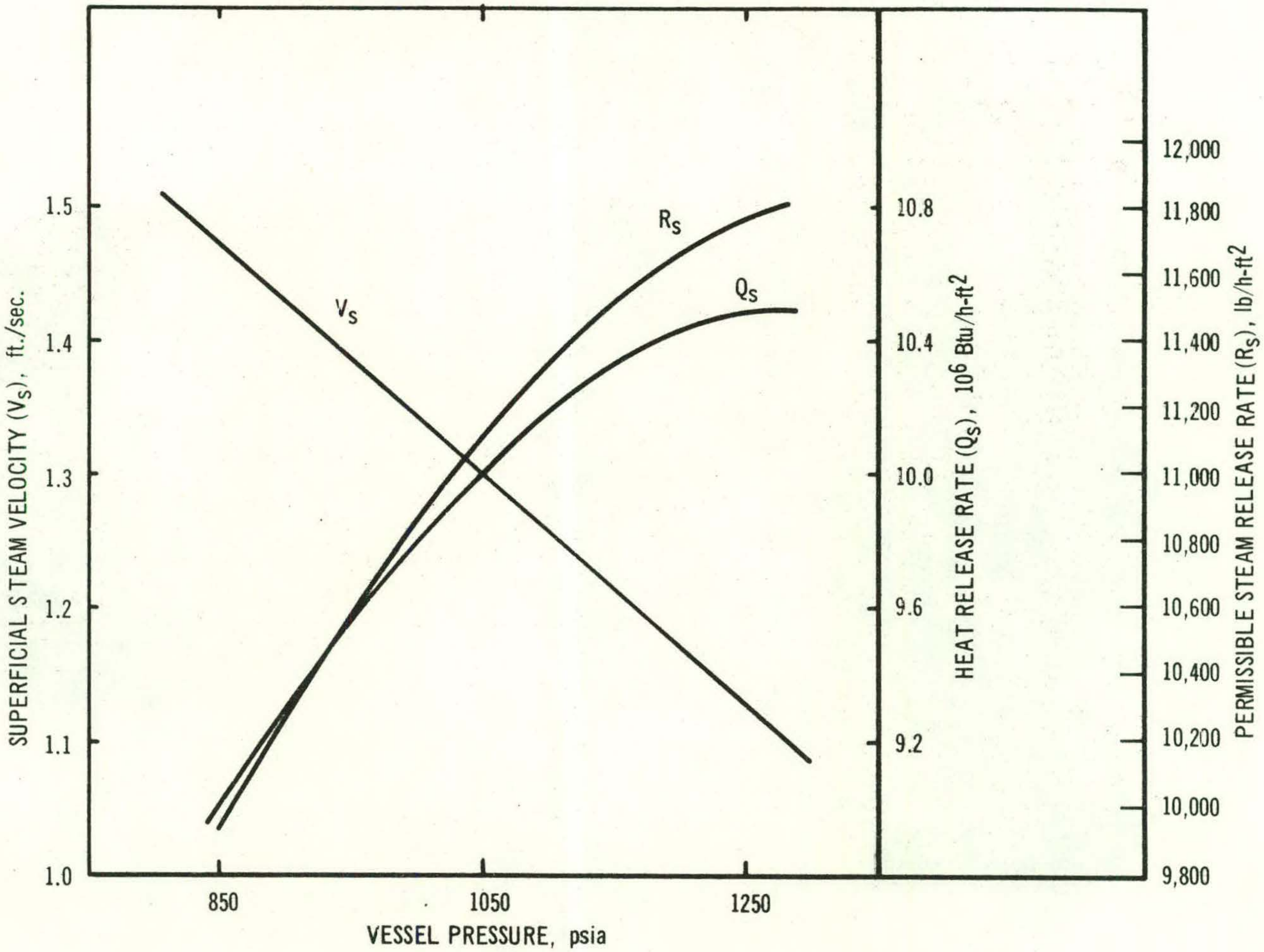

Figure 5-33. Superficial Steam Velocity, Permissible Steam Release Rate and Heat Release Rate vs Reactor Pressure

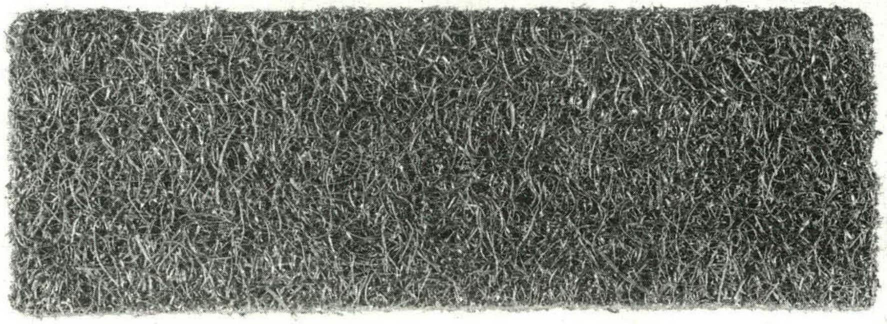

Figure 5-34. Photograph of Sintered Random Mesh, Stainless Steel Insulation

Figure 5-35. Photograph of Embossed Laminated Stainless Steel Foils

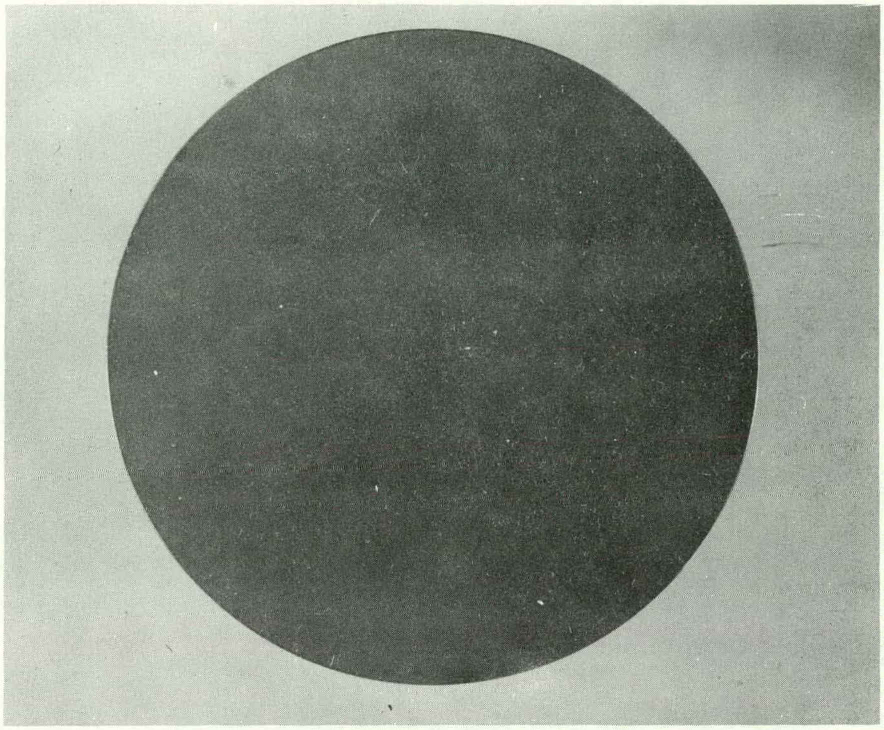

Figure 5-36. Photograph of Sintered Powder Porous Stainless Steel Sample

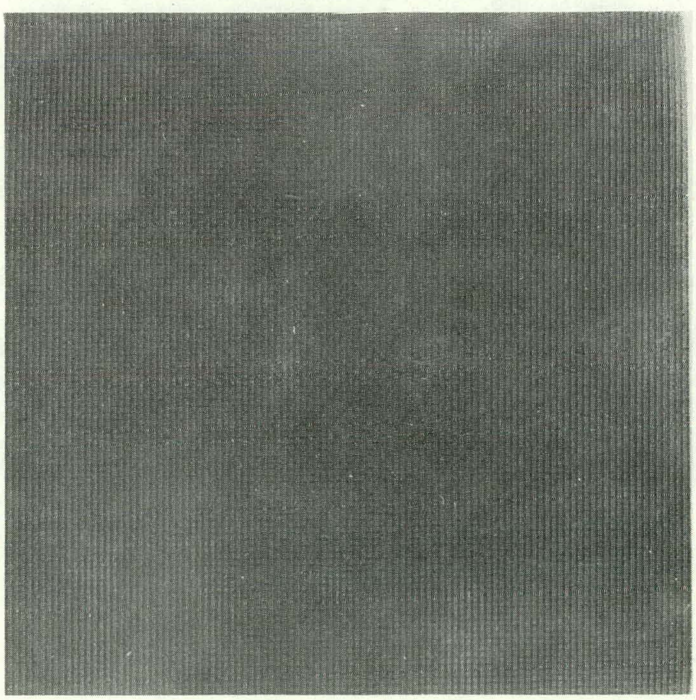

Figure 5-37. Photograph of Woven Mesh Sintered Stainless Steel Sample

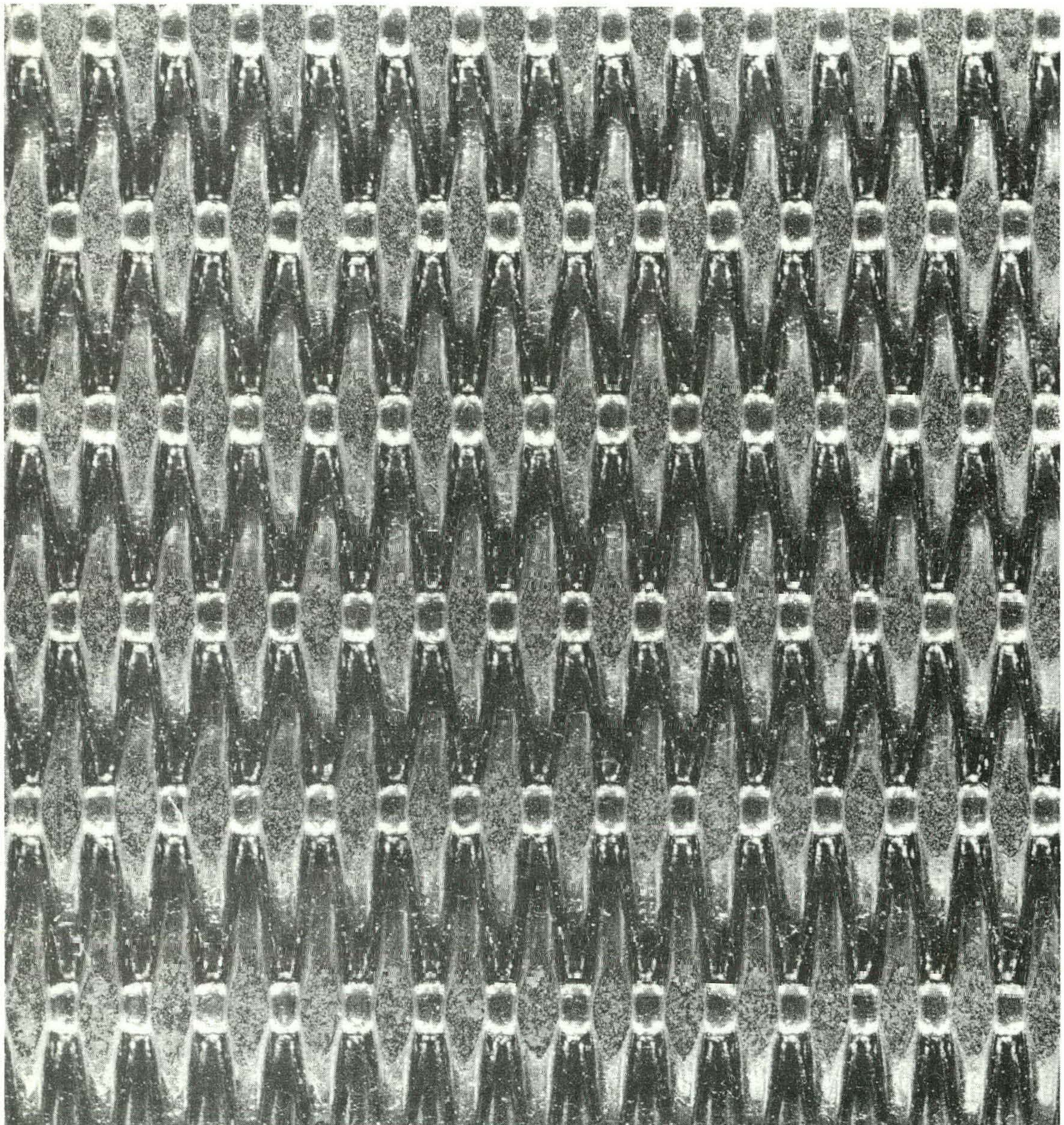

Figure 5-38. Close Up of Woven Sintered Stainless Steel for Transpiration Cooling

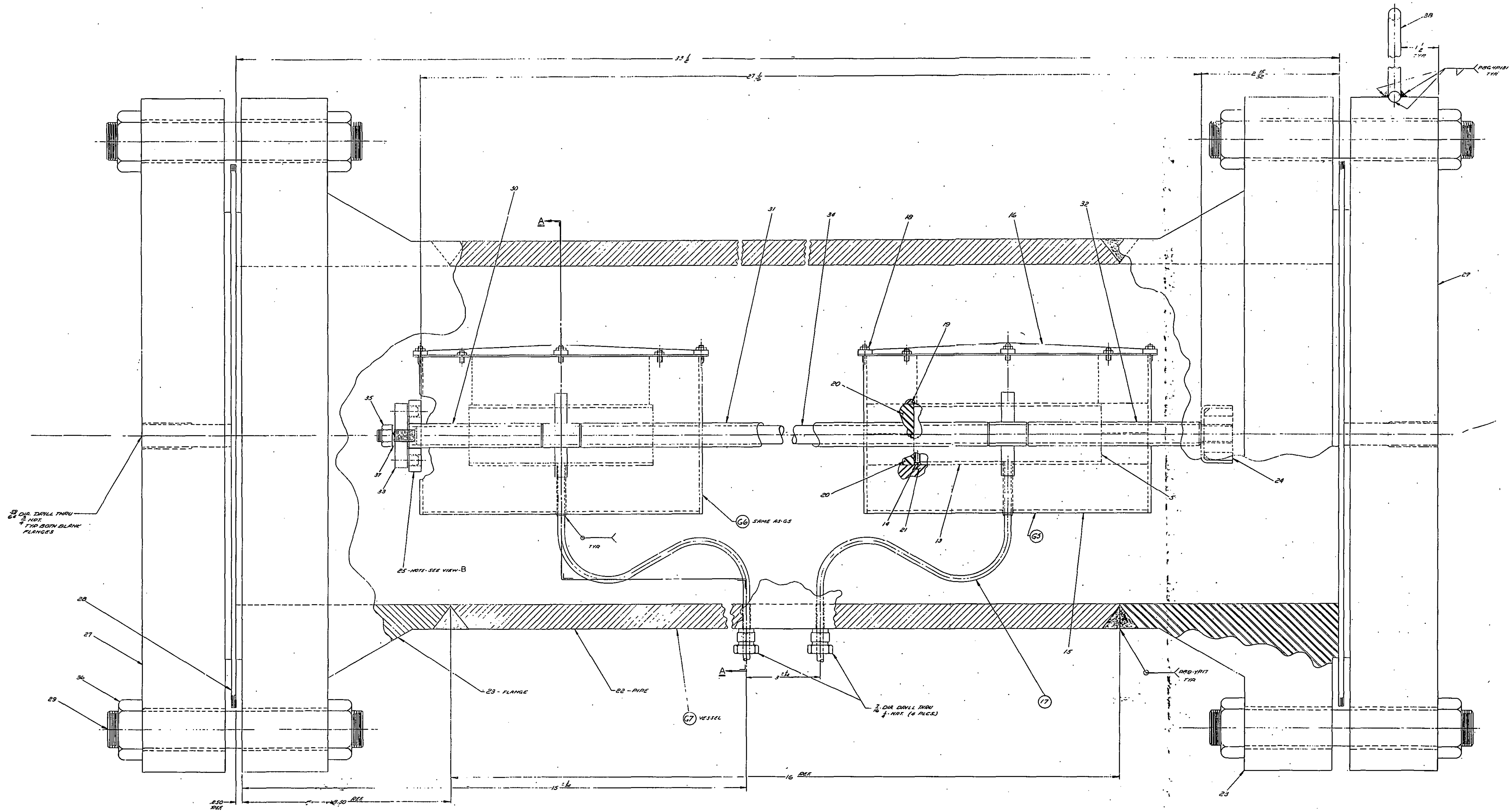

Figure 5-39. Internal Device for Static Cooling Test

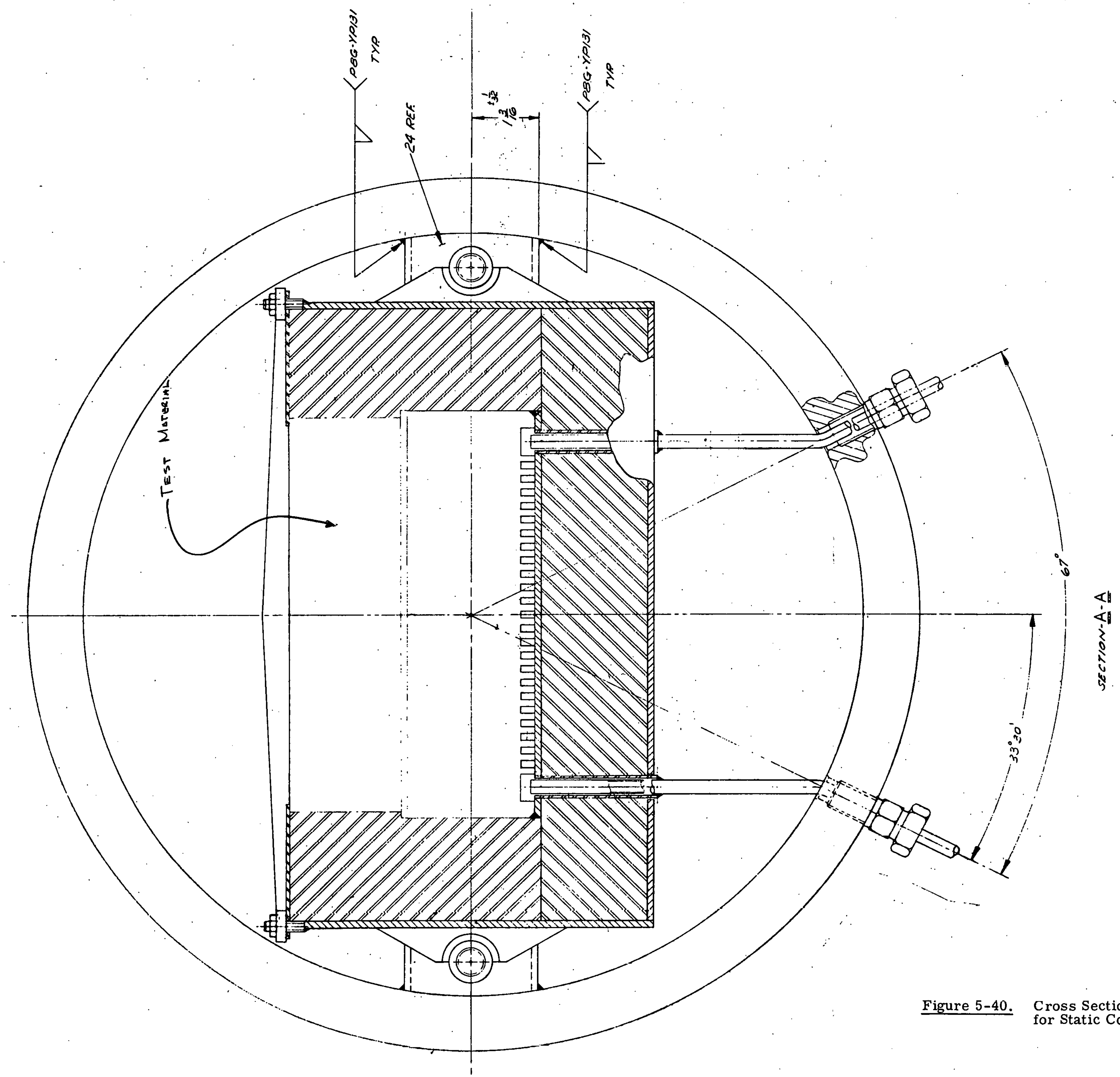

Figure 5-40. Cross Section of Internal Device for Static Cooling Test

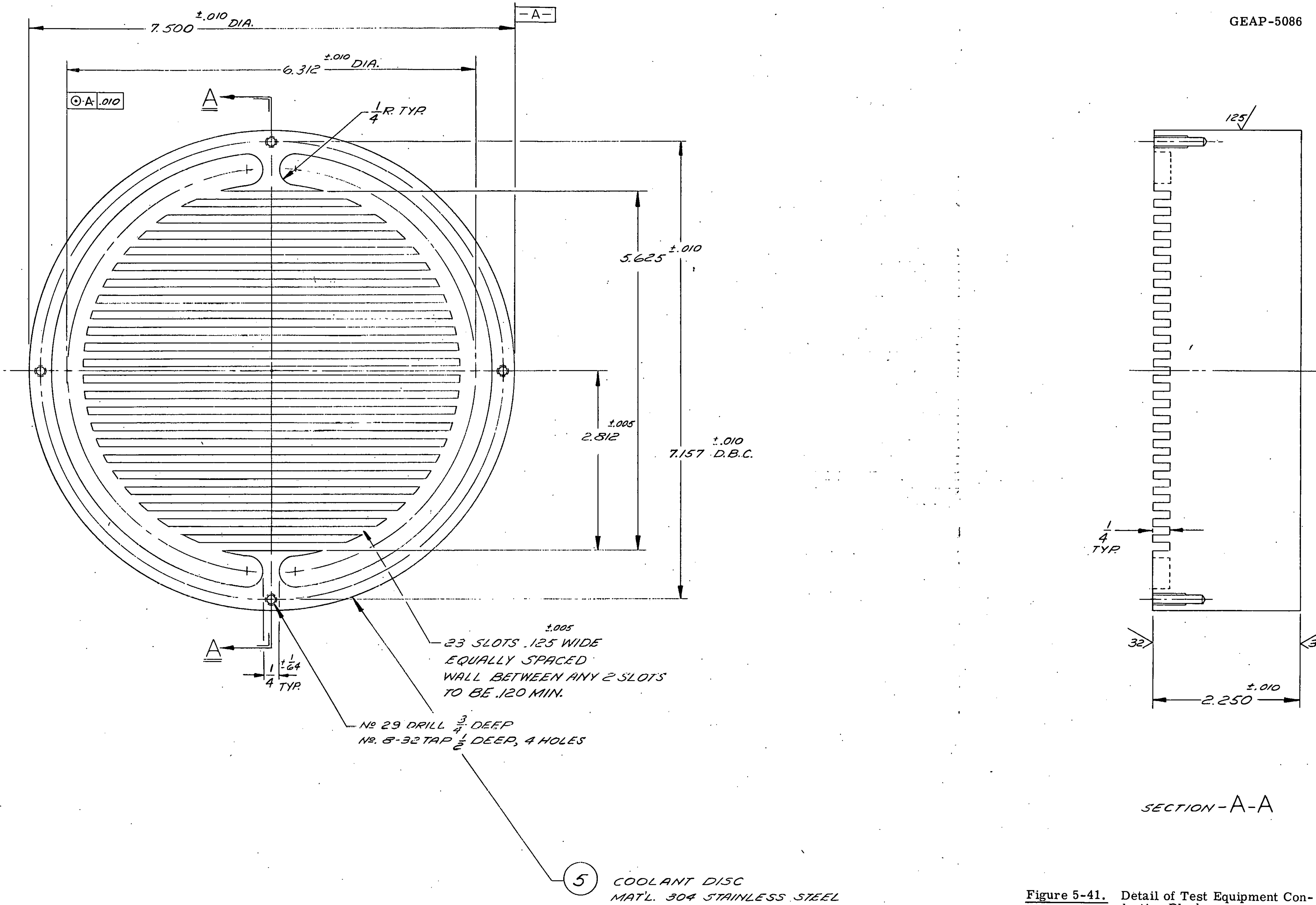

Figure 5-41. Detail of Test Equipment Conduction Block

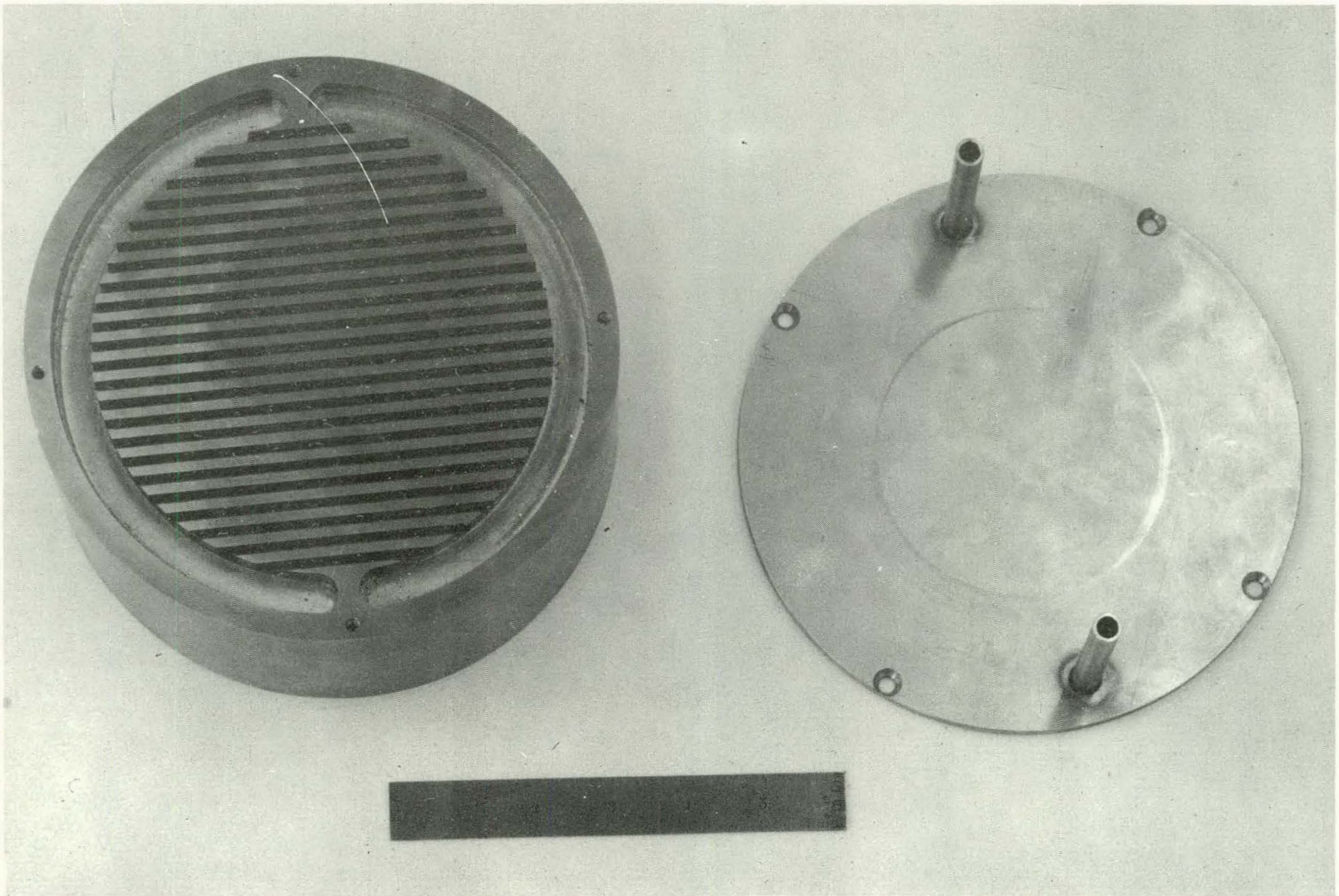

Figure 5-42. Photograph of Conduction Block

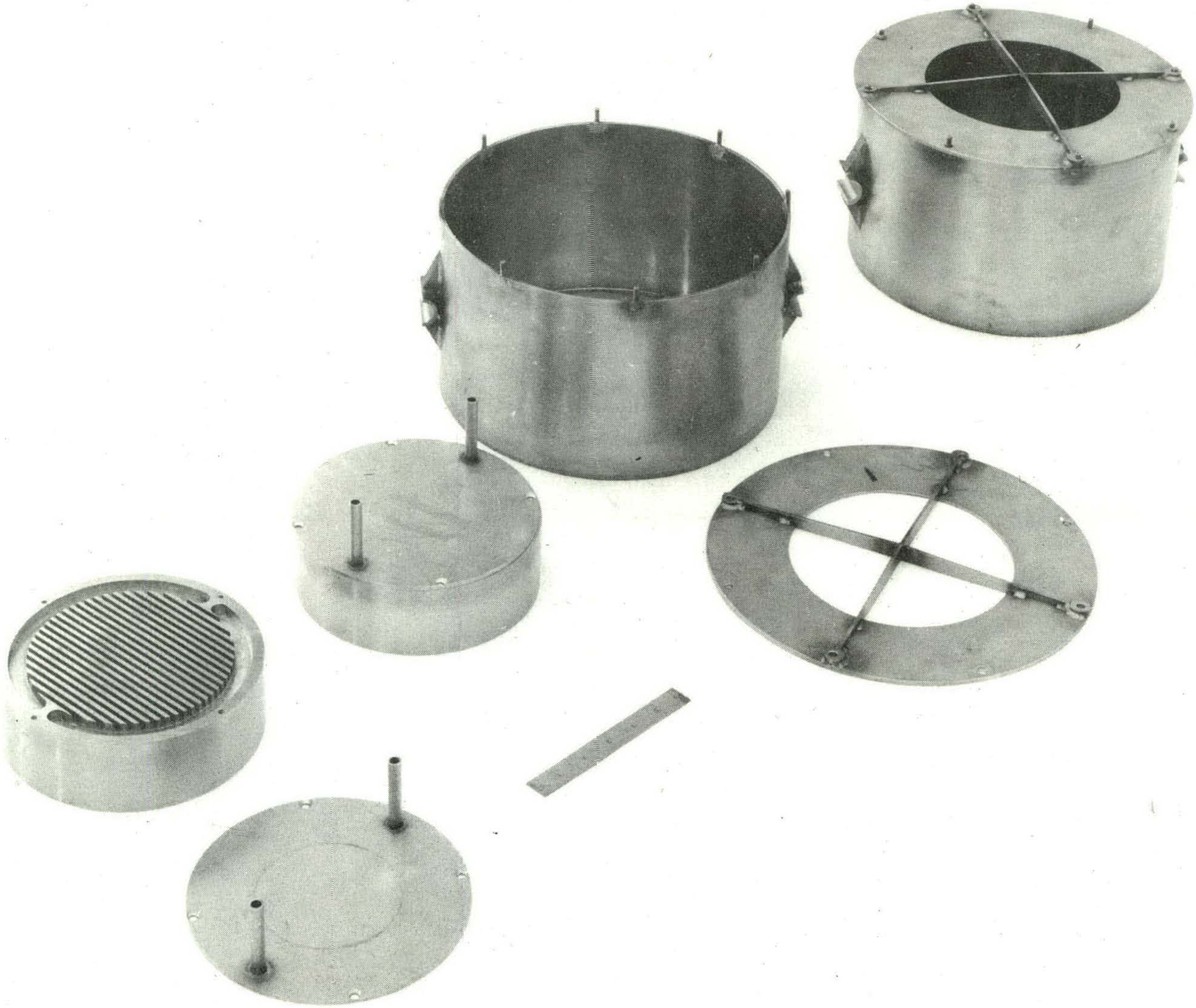

Figure 5-43. Photograph of the Heat Transfer Device Including Insulation Sample Container

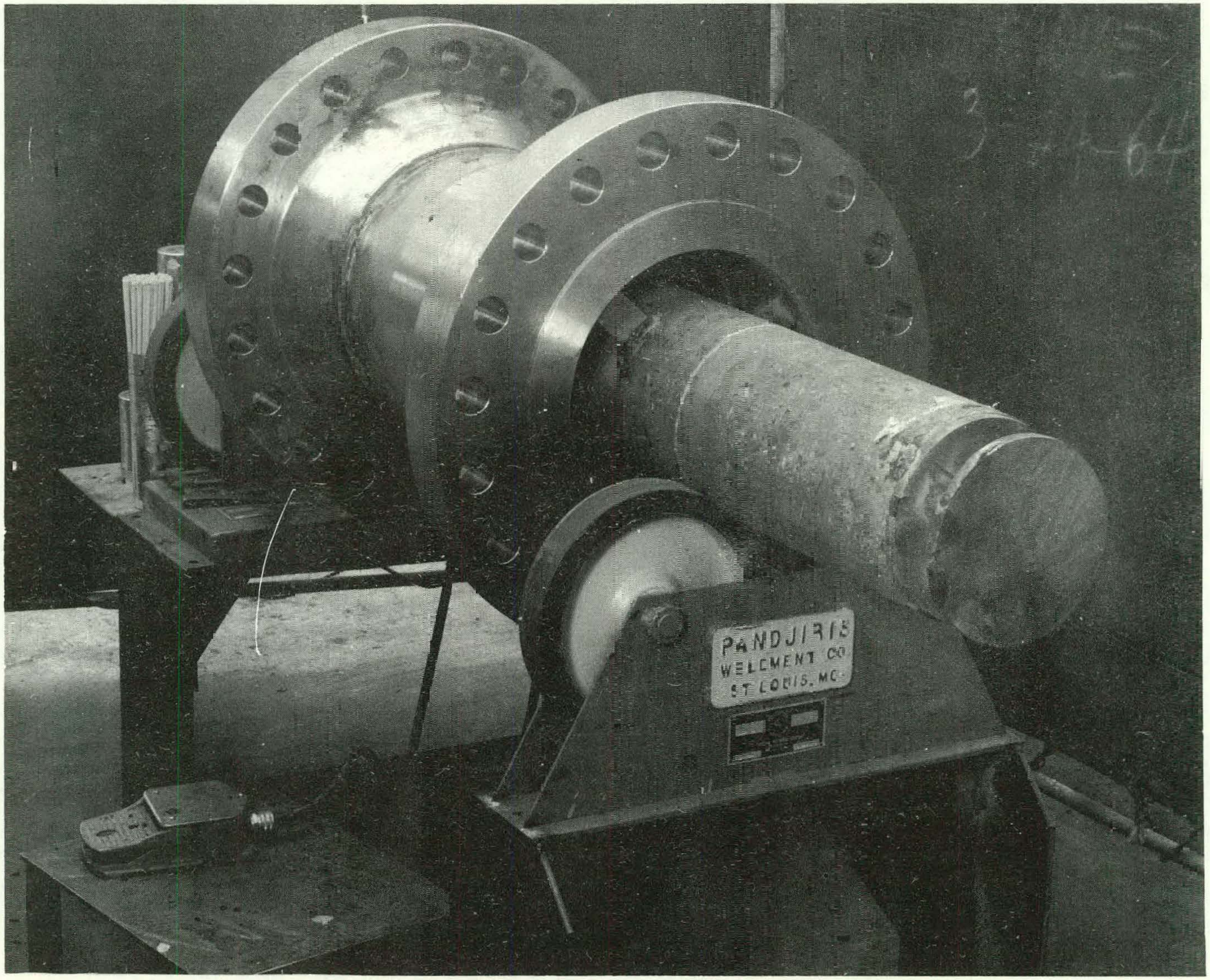

Figure 5-44. Photograph of 14-inch I. D. Pressure Vessel During Construction

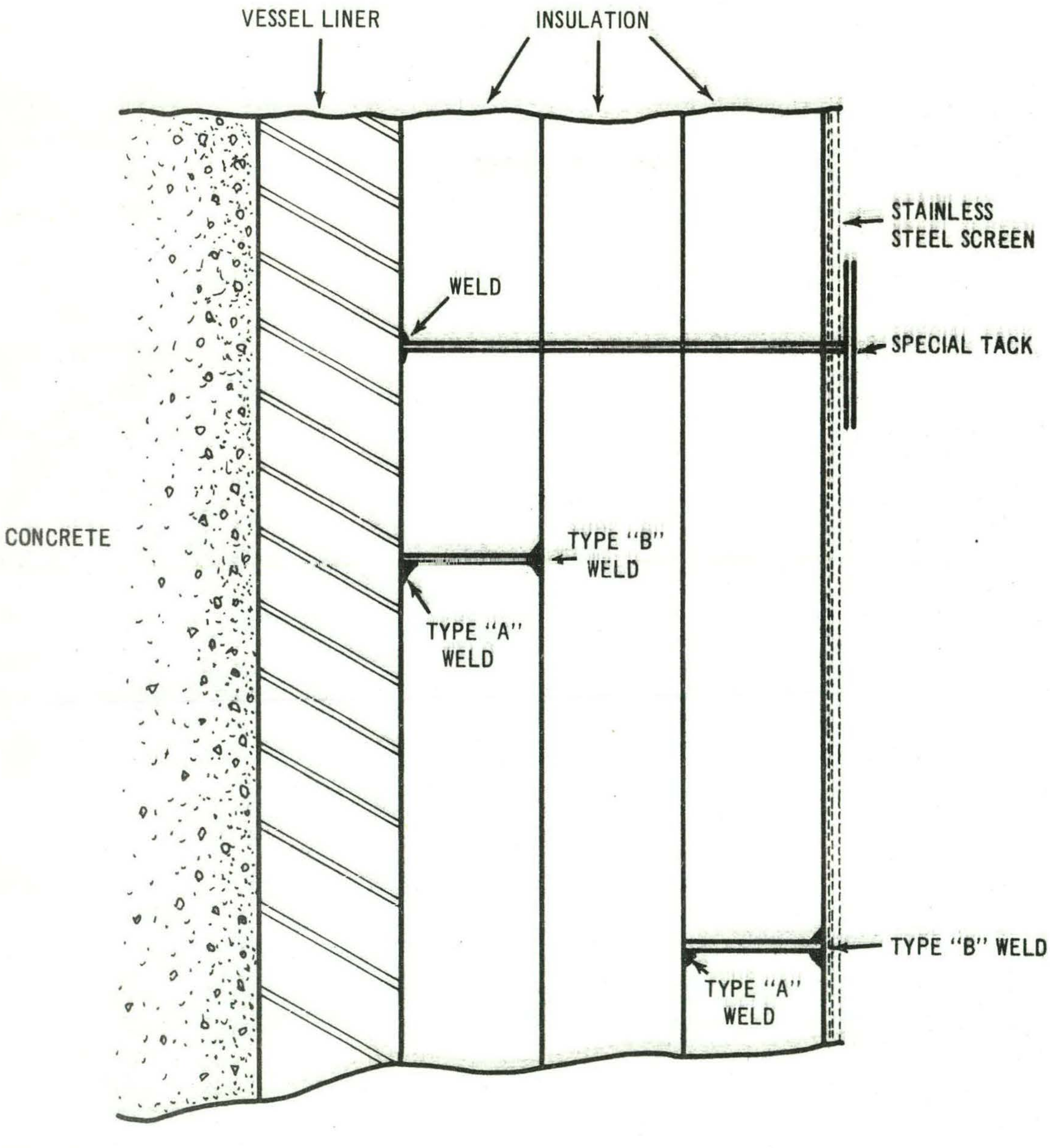

Figure 5-45. Details of Insulation Installation Techniques

PRINCIPAL INVESTIGATORS

P. M. Murphy Project Engineer
C. E. Boardman
G. Boggio*
R. C. Brandt**
W. J. Clabaugh
J. E. Hench
S. Levy
G. D. Matty
W. A. Sangster
J. M. Sorensen

*Euratom Participant
**Elecricité de France Participant

DISTRIBUTION LIST

USAEC San Francisco Operations Office 2111 Bancroft Way Berkeley 4, California Attn: Director, Contracts Division	23
USAEC San Francisco Operations Office 2111 Bancroft Way Berkeley 4, California Attn: Director, Reactor Division	2
U.S. Atomic Energy Commission Division of Reactor Development & Technology Washington, D. C. 20545	
Chief, Water Reactors Branch	2
Chief, Desalination Branch	1
Chief, Gas-Cooled Reactors Branch	1
Chief, Fuels & Materials Development Branch	1
Chief, Nuclear Safety Research & Development Branch	1
Chief, Nuclear Safety Analysis & Evaluations Branch	1
Assistant Director for Foreign Activities	1
Chief, Reports and Statistics Branch	1
U.S. Atomic Energy Commission Advisory Committee on Reactor Safeguards Washington, D.C. 20545 Executive Secretary	1
U.S. Atomic Energy Commission Division of Construction Washington, D.C. 20545	
Director	1
Chief, Engineering Branch	1
U.S. Atomic Energy Commission Division of Internal Affairs Washington, D.C. 20545 Director	1
U.S. Atomic Energy Commission Division of Labor Relations Washington, D.C. 20545 Director	1
U.S. Atomic Energy Commission Asst. General Counsel for Patents Washington, D.C. 20545	1
U.S. Atomic Energy Commission Division of Naval Reactors Washington, D.C. 20545 Chief, Reactor Engineering Branch	1
U.S. Atomic Energy Commission Oak Ridge Operations Office Oak Ridge, Tennessee 37831 Director, Reactor Division	2
U.S. Atomic Energy Commission Chicago Operations Office Argonne, Illinois 60439 Director, Reactor Division	1

DISTRIBUTION LIST (Cont)

U.S. Atomic Energy Commission Division of Technical Information Extension Oak Ridge Operations Office Oak Ridge, Tennessee 37831	3 + Negatives
Allis-Chalmers Manufacturing Company 6935 Arlington Boulevard Bethesda, Maryland 20014 Attn: General Manager	1
American Society of Mechanical Engineers 345 East 47th Street New York, New York 10017 Attn: J. D. Wilding	1
Bettis Atomic Power Laboratory P.O. Box 79 West Mifflin, Pennsylvania 15122 Attn: B. P. Langer	1
College of Engineering University of California Berkeley, California 94720 Attn: T. Y. Lin	1
General Atomic Division of General Dynamics Corp. P.O. Box 608 San Diego, California 92112 Attn: R. Marsh	1
Oak Ridge National Laboratory Oak Ridge, Tennessee Attn: M. Bender	1
Oak Ridge National Laboratory Oak Ridge, Tennessee Attn: I. Spiewak	1
Raymond C. Reese Associates 300 Sandusky Street Toledo, Ohio Attn: R. C. Reese	1
Westinghouse Electric Corporation P.O. Box 355 Pittsburgh, Pennsylvania Attn: General Manager	1
Mr. Francois Germain Assistant General Manager Societe d'Etudes & d'Equipments d'Entreprises 9, Rue Sextius-Michel Paris 15e, France	5